OMLESCA: Optimization of Modular Liquid Expulsion Systems for CubeSat Applications

a project presented to
The Faculty of the Department of Aerospace Engineering
San José State University

in partial fulfillment of the requirements for the degree
Master of Science in Aerospace Engineering

by

Travis T. George

May 2024

approved by

Dr. Maria Chierichetti
Faculty Advisor

SAN JOSÉ STATE
UNIVERSITY

ABSTRACT

OMLESCA: Optimization of Modular Liquid Expulsion Systems for CubeSat Applications

Travis T. George

Since the satellite market shifted towards using CubeSats in the early 2000's, there is currently a need for propulsion systems that require less volume while still maintaining high enough thrust for orbital maneuvers. A major part of the propulsion system consists of the pressure vessel where the propellants and oxidizers are stored. Depending on the propellant used, pressure vessels are often times made from a minimum of two, for both propellant and oxidizer, or even three different tanks if a pressurant gas is required for expulsion. Depending on the mission duration, these vessels use a large portion of the small amount of volume available in CubeSats. The goal for OMLESCA is to decrease the overall volume and mass required for a CubeSat propulsion system. This is done by first selecting a propellant called High-Test Hydrogen Peroxide, which is popular for its ability to perform as both a propellant and its own oxidizer. This automatically eliminates the requirement of two vessels for the propellant and oxidizer. Secondly, the vessel itself combines the propellant with the pressurant into one tank which reduces the overall volume even further. Since there is little to no gravity in space, the propellant needs a driving action to force the propellant into the thruster. OMLESCA uses a rectangular tank that utilizes a piston type expulsion system which is driven by nitrogen gas. This makes the overall design unique because the round piston, bored from the rectangular tank, leaves corners of unused areas which can additionally be bored as the shape of triangles. These triangular pockets store nitrogen gas and, with clever internal holes and solenoids, drive the piston to deliver the propellant. The propellant output requires the pressure to remain at 250 psi for optimal thrust from a 1 N thruster. The pressurant gas is held at 750 psi and regulated at 250 psi to negate as much effect of blowdown as possible. To prepare for integration into a Falcon 9 rideshare CubeSat launcher, the system must undergo static structural and vibrational analyses to validate the system can withstand launch and space environments. From the static structural analysis, it was found that the tank could well withstand the pressure of 750 psi and had a safety factor of 1.9. Additionally, modal analysis found the lowest mode of the system to be at a frequency of 4062 Hz which is well above the required 40 Hz. Using the flight envelope given by the Falcon 9 rideshare guide, harmonic analysis found that the largest displacements occurred at 4297 and 6523 Hz but only contributed to a maximum displacement of 0.007 mm. This displacement is basically negligible for this case. Random vibration analysis predicted a 66.269% probability the deformation would remain under 0.000104 mm and a 99.73% probability to remain under 0.000314 mm. From these analyses, the propellant tank was found to be ready for further environmental thermal vacuum testing to prepare for integration into a CubeSat for launch.

Acknowledgements

I would like to thank Dr. Chierichetti for her guidance and advice throughout this project. Although I was unfortunate not to have her as a professor for any of my undergraduate or graduate courses, I was able to gain much knowledge from her expertise during our advisory meetings.

In addition, I want to send my utmost gratitude to my undergraduate senior design team for their contribution towards the early stages of this project. Their inspiration gave me motivation to continue forward with this design and expand it further. My senior design team deserves the opportunity to watch the tank undergo proof burst testing because I had promised them that they would get to see the tank explode at its maximum pressure. Thank you again to Mark Chahal, Joel Fajardo, Andrew Zarate, Destiny Hernadi, and Surya Shivakumar.

Lastly, I would like to thank my parents Craig and Debbie, and my girlfriend Kailee for the support while finishing my master's degree.

i. Table of Contents

ii. List of Tables

iii. List of Figures

iv. List of Acronyms

Symbol	Definition
2D	Two Dimensional
3D	Three Dimensional
AF-M315E	Advanced Spacecraft Energetic Non-toxic Propellant
CAD	Computer Aided Design
CFD	Computational Fluid Dynamics
CFM	Cubic Feet per Minute
CPU	Central Processing Unit
dB	Decibel
DDAM	Dynamic Design Analysis Method
EMISM	Electromagnetic Interference Safety Margin
FEA	Finite Element Analysis
G or g	Gravity
GB	Gigabyte
GNC	Guidance Navigation and Control
HNP225	Highly stable Non detonating Propellant
Hz	Hertz
ID	Inner Diameter
In	Inches
in^2	Inches Squared
In lb	Inch Pound
Isp	Specific Impulse
ISS	International Space Station
JWST	James Webb Space Telescope
K	Kelvin
Kg	Kilograms
L	Liter
Lb	Pounds
LE	Low Earth Orbit
LEO	Low Earth Orbit
LMP-103S	Ammonium Dinitramide based Liquid Propellant

Symbol	Definition
MEOP	Maximum Expected Operating Pressure
MEO	Medium Earth Orbit
mJ	Millijoules
mN	MilliNewtons
MPa	Megapascals
m/s	Meters per Second
N	Newton
NPT	American National Pipe Tapered Thread
ODE	Ordinary Differential Equations
PLx	Payload X Direction
PLy	Payload Y Direction
PLz	Payload Z Direction
PDE	Partial Differential Equations
Psi	Pounds per Square Inch
PSD	Power Spectral Density
RAM	Random Access Memory
RCS	Reaction Control System
RF	Radio Frequency
R134a	Tetrafluoroethane Refrigerant
R236fa	Hydrofluorocarbon Refrigerant
Sec	Seconds
SPL	Sound Pressure Level
Sqft	Square Foot
SS	Stainless Steel
Torr	Unit of Pressure
TV	Television
TVAC	Thermal Vacuum
U	Unit of CubeSat measurement; a 10cm cube

1. Introduction

1.1 Motivation

In recent years the new frontier of exploration has been all about space, sparked from the findings of planetary bodies from the Hubble space telescope and JWST. Ever since the start of the 2000's, universities and commercial space companies have shown a large increase in the desire to send satellites into orbit. This desire was once nearly impossible to fulfill due to the high costs of sending spacecraft into orbit. For example, JWST cost a total of about $10 billion, while the Hubble telescope cost $2 billion at launch, but due to needing multiple repairs, ended up costing a total of $16 billion. With launches costing this much money, it is clear why not very many companies are able to send their technology into space. While cost is a limiting factor, it is actually no longer the biggest hurdle. In fact, thanks to the collaboration of the two professors Jordi Puig-Suari and Bob Twiggs, the solution to these expensive launches was created. In 1999, they introduced the CubeSat, a class of small satellites that cultivated a new standardized size range and unit of measurement [1]. With the addition of the CubeSat, a new revolution of space technology was started. In figure 1.1, the number of CubeSats launched versus year for mission type can be seen.

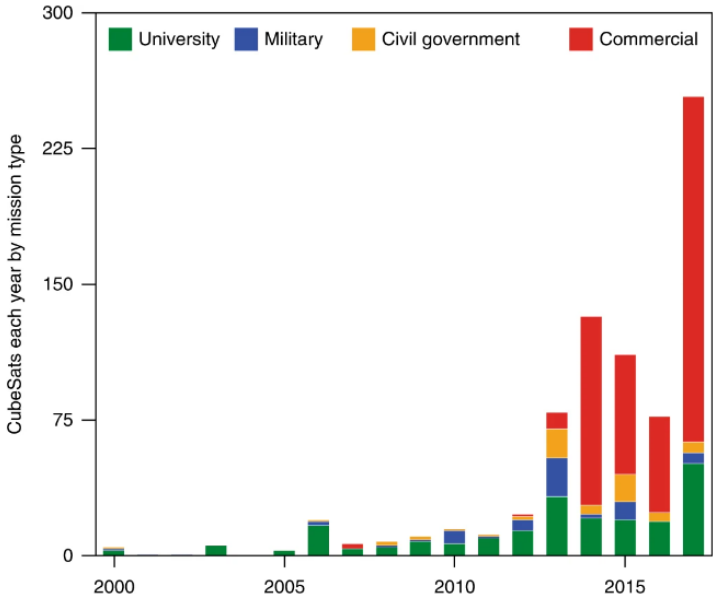

Figure 1.1 Number of CubeSats launched by mission type per year [2]

Since the size of the spacecraft was smaller, the technology on board, such as the propulsion system, also needed to decrease. Propulsion in space requires a different approach to be capable of producing thrust when compared to airbreathing jet propulsion as an example. Due to the spacecraft being in microgravity, liquid propulsion systems require the propellant to be positively expelled from a fuel vessel to the thruster. These expulsion devices are oftentimes

very complex, bulky, and expensive to manufacture. Every CubeSat that uses liquid propulsion needs a fuel vessel that is capable of storing and delivering propellant on demand, but also utilizes the least amount of volume and weight.

1.2 Literature Review

1.2.1 CubeSats

1.2.1.1 Introduction

CubeSats are a magnitude smaller than satellites such as Hubble and JWST, which both are around the size of a bus. They are restricted to standardized sizes of 1U, 1.5U, 2U, 3U, 6U, and 12U. The unit "U" refers to a 10cm cube where each 1U has a maximum mass of 2 kg. This relationship can be seen in figure 1.2 below.

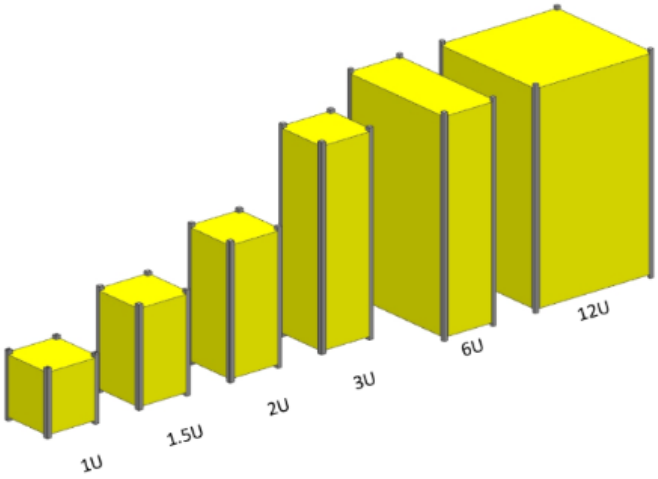

U Configuration	Mass [kg]
1U	2.00
1.5U	3.00
2U	4.00
3U	6.00
6U	12.00
12U	24.00

Figure 1.2 CubeSat sizing comparison with size to maximum mass [1]

The intent of the development of CubeSats was to reduce cost and development time, increase accessibility to space, and sustain frequent launches [1]. CubeSats are continuously growing in popularity and because of this, parts made specifically for them are becoming more readily available and at a lower cost. In addition to the standardization of size, companies such as Nanoracks have also been able to develop a set of standard deployment systems for use on rocket payloads, and dispensers on the ISS. Advancements in technology such as precision pointing, compact sensitive detectors and the miniaturization of propulsion systems has made CubeSats become feasible [2]. The same motive is seen in modern technology where the common goal is to make the best sensors and cameras fit inside the smallest products. An example of this is small, embedded cameras that started as expensive gadgets but driven by smartphones, became progressively cheaper, smaller, and better performing, enabling them to be used in everything from cars to drones and even CubeSats [2].

1.2.1.2 Example Missions

Rocket launches into orbit cost a lot of money, sometimes this can be millions to even billions of dollars. With the intent of making CubeSat missions more affordable, these high-cost launches make this idea of affordability difficult to achieve. A solution to this is to launch CubeSats as secondary payloads with a large payload that has extra space in the fairing. In this extra space, special deployment mechanisms are integrated so that they are mounted to the main payload structure. A commonly used deployment mechanism is made by Nanoracks that holds the CubeSats until they are ready to be deployed. To ensure safety, the CubeSats are fully disabled and self-contained until deployment so that there is no risk to the launch vehicle or main payload. Nasa has contributed to the development of CubeSats by starting the CubeSat launch initiative that subsidizes the launch cost for universities, high schools, and non-profit organizations [2]. CubeSats are commonly launched into LEO and MEO orbits, but efforts are being made to launch them further for missions to the moon and beyond.
Missions for CubeSats beyond Earth orbit include [2]:

Moon

- LunaH-Map | CubeSat to map hydrogen enrichments within permanently shadowed regions of the lunar south pole [3].
- Lunar Flashlight | CubeSat that will use infrared lasers and an onboard spectrometer to map ice in permanently shadowed regions near the Moon south pole [4].
- Lunar IceCube | CubeSat mission to study the distribution of water and organic volatiles on the Moon [5].

Mars

- MarCo | First interplanetary CubeSat designed to monitor InSight for a short period around landing and to demonstrate potential future capability [6].

Asteroid

- NEA-Scout | Serves as a robotic reconnaissance mission to fly by and return data from an asteroid representative of near-Earth asteroids that may one day be human destinations [7].

1.2.2 Propulsion Systems

Since CubeSats are smaller than traditional satellites, the components must also be smaller. This is no exception for the propulsion system. CubeSat propulsion systems are a magnitude smaller, and generally have a maximum thrust output of 10 N. The thrust is more commonly within 1 N range, but after blowdown, a propellant pressure drop that decreases the thrust output, the thrust ends up in the milli-Newtons.
Common thruster types used:

- Green Monopropellant
- Bipropellant
- Cold/Warm Gas
- Resistojet
- Electric Ion Propulsion

1.2.2.1 Green Monopropellants

Green Monopropellants are currently considered as enabling technology that is revolutionizing the development of high-performance space propulsion, especially small sized spacecraft [8]. A monopropellant is considered green if it is considered safe, non-toxic, and does not produce any harmful chemicals as a byproduct of decomposition. The main focus of using green propellants is to lessen the harmful effects on the environment by replacing the commonly used, but very nasty, hydrazine propellants. Hydrazine has been used as a propellant since the 1930's because it has great properties useful for rockets, but is notorious for being extremely toxic, carcinogenic, corrosive, flammable, and explosive [9].
Some examples of green monopropellants are:

- AF-M315E | Hydroxylammonium Nitrate, Adiabatic Flame Temperature: 2100 K, Isp: 270 sec [8]
- LMP-103S | Ammonium Dinitramide, Adiabatic Flame Temperature: 1900 K, Isp: 250 sec [8]
- HNP225 | Hydroxyl Ammonium Nitrate, Adiabatic Flame Temperature: 1000 K, Isp: 200 sec [8]
- HTP | Hydrogen Peroxide, Adiabatic Flame Temperature: 2600 K, Isp: 160 sec [8]

Knowing the adiabatic temperature of a propellant is important because it drives the material choice of the nozzle to select one with high enough thermal properties. The adiabatic temperature vs. Isp of the green monopropellants can be seen in figure 1.3.

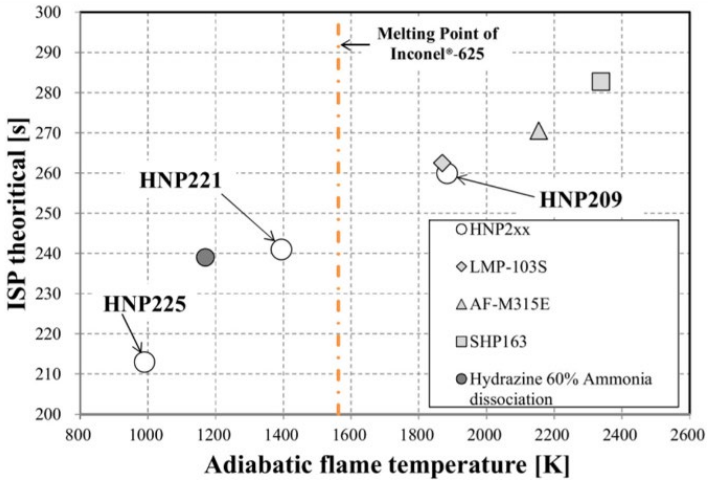

Figure 1.3 Adiabatic flame temperature vs. Isp [8]

1.2.2.2 Bipropellants

Bipropellant systems utilize the energy produced from the combustion of two combined propellants. These propellants usually involve a fuel and oxidizer which work well in vacuum missions due to the presence of the oxidizer. Depending on the propellants used, the reaction either needs to be started with an ignition system, or solely by mixing the agents due to their hypergolic properties. This high-temperature, high-pressure gaseous mixture is expanded using a converging–diverging nozzle to create a high velocity exhaust stream [10]. Bipropellants are generally seen in launch vehicles due to their high thrust outputs at low altitude, and versatility for use in vacuum.

1.2.2.3 Cold/Warm Gas

Cold and warm gas propulsion systems are commonly used in RCS systems for spacecraft that need small orientation changes. It is primarily used when precise vehicle pointing is needed, especially for docking procedures on the ISS. The cold gas system involves the release of a stored pressurized gas where the energy from the release accelerates the spacecraft. In addition, the warm gas systems involve using a heater to warm the gas before its release to increase the energy output. The amount of energy released is usually pretty small and will not be used for long duration firing periods. Typical propellants used are isobutane, the refrigerants R236fa and R134a, and sulfur dioxide [10].

1.2.2.4 Resistojet

Resistojet propulsion utilizes electrothermal energy to decompose a propellant gas. They typically are designed in a way that allows the propellant to pass over as much heated surface area as possible. Typical configurations electrically heat the surface to increase the propellant gas

beyond the stagnation temperature of the purely chemical propulsion system, and therefore augment the resulting exhaust velocity after expansion [10].

1.2.2.5 Electric Ion Thruster

Electric Ion thrusters use the acceleration of ions between the potential difference of charged surfaces. One of the ways to do this is to heat a material in the cathode, such as Lanthanum Hexaboride (LaB6), until it reaches its thermionic emission temperature which causes electrons to boil out of the material. An inert gas, usually noble gases, is pumped at a low mass flow rate through the cloud of electrons which bombards the neutral gas atoms to create ions and additional electrons. This process starts a chain reaction that generates more and more ions that are attracted to plates or grids with a lower potential energy. As the ions are ejected from the thruster, an external cathode is needed to neutralize the ion cloud. The two common ion thrusters are gridded and hall effect thrusters. Recent developments in miniaturized ion engines make use of RF ionization, obviating the need for an internal electron emitter [10].

1.2.3 Expulsion Systems

Propulsion systems, specifically monopropellant systems, consist of a propellant tank, pressurant tank, various valves and solenoids, piping, and the nozzle. While solenoids and valves are continuously getting smaller, bulky propellant and pressurant tanks are what need innovation. The propellant tank, which is generally referred to as the expulsion device, uses a pressurized inert gas such as helium or nitrogen from a separate pressurant tank to compress the expulsion device to push out the propellant. While there are many different ways this can be done, the three main types of expulsion are:

- Bladder expulsion
- Diaphragm expulsion
- Piston expulsion

1.2.3.1 Bladder Expulsion

Bladder expulsion systems work just like a balloon inside of a metal tank. A flexible membrane inside the tank is what holds the propellant and separates it from the pressurant. With the propellant filled bladder, the external pressurant pressurizes the outer portion of the bladder and causes the compressed propellant to flow out of a valve. Due to the flexibility of the bladder, the shape of the tank is the ultimate factor that dictates the shape of the bladder. Although this shape has its limitations, if a bladder is too small it risks overstretching, additionally, if the bladder is too big it risks creasing [11]. Overstretching and creasing are potentially catastrophic because they can lead to premature bladder failures by popping or ripping. The goal of the bladder is to achieve optimum efficiency by holding it as close to the internal volume of the tank with

propellant and expelling the same amount to the thruster. The shapes of these tanks generally are spherical because it ensures even pressure on the bladder and the least number of edges to cause ripping or creases. Different illustrations of filling bladder tanks can be seen in figure 1.4.

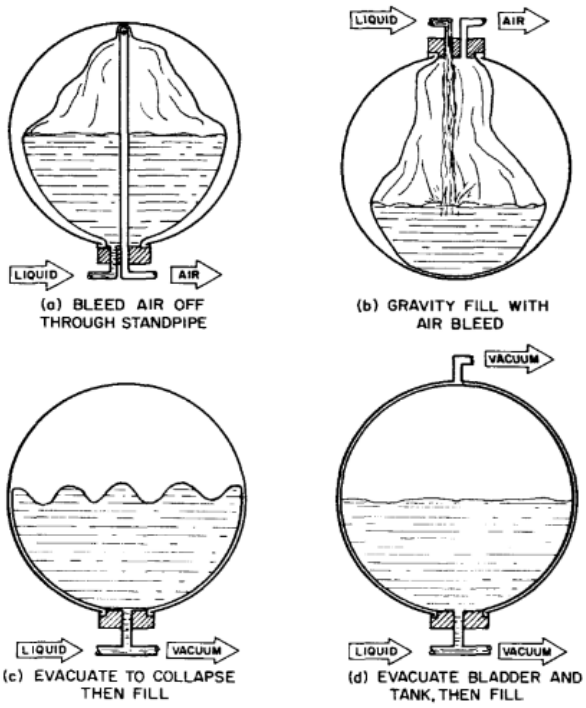

Figure 1.4 Bladder tank filling techniques [11]

1.2.3.2 Diaphragm Expulsion

Diaphragm expulsion works very similar to bladder due to the presence of a membrane that separates the propellant and pressurant. The major difference between the diaphragm and bladder is that the diaphragm can fully reverse itself and is also internally pressurized. Diaphragm tanks can either be symmetric so that their reverse is a mirror image, or they can start as an intermediate shape and be formed by pressure into a completely different shape [11]. An example of how the diaphragm reverses itself when filled can be seen in figure 1.5.

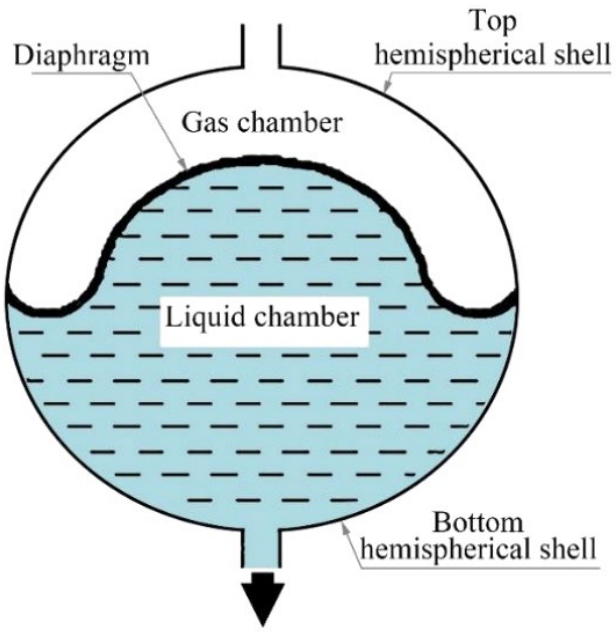

Figure 1.5 Diaphragm expulsion tank [12]

1.2.3.3 Piston Expulsion

Piston expulsion uses a different approach than the bladder or diaphragm. It works very similar to how an automotive piston would work inside of an engine. The piston sits inside of a cylinder, both of them perfectly round and polished smooth. In between the piston and cylinder wall sits a seal to prevent the upper portion from mixing with the bottom portion. These seals can be made of metal, rubbers, or bellows dependent on the type of propellant used. For the system to work properly, the piston seals must prevent leakage while allowing the system to be dynamic. Under the piston is where the propellant is held, and at the bottom is the exit where the propellant is expelled. Above the piston is the pressurized inert gas which constantly exerts pressure on the propellant to hold it in place for when the exit valve is opened. This constant pressure prevents the propellant from sloshing around inside the tank. Pistons are chosen to be round for the best sealing capability and lengthwise may be flat, cylindrical, concave, or convex [11]. Using a center guide through a flat piston is generally required to lessen the possibility of getting stuck from the piston cocking inside the cylinder. Both the piston and cylinder are generally made from metallic materials, specifically dependent on the propellant it intends to store. An example of a concave piston and cylinder can be seen in figure 1.6.

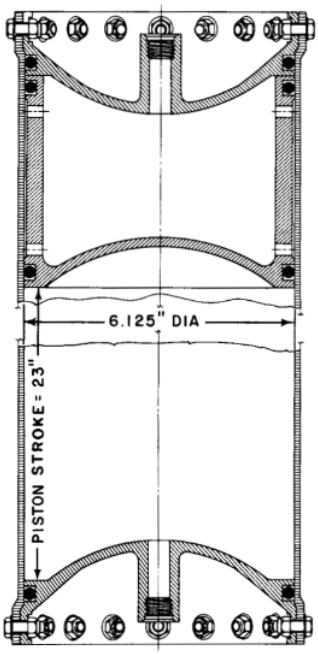

Figure 1.6 Hydrazine Piston expulsion tank [11]

1.2.3.4 Mission Propulsion/Expulsion Systems

Analyzing the CubeSats mentioned in section 1.2.1.2, a list of the type of propulsion system they had and what expulsion mechanisms they used can be seen below.
The propulsion/expulsion systems were:

- LunaH-Map | Gridded Ion Thruster, Solid Iodine propellant with valve [3]
- Lunar Flashlight | Green Monopropellant, Titanium diaphragm with AF-M315E [4]
- LunarIceCube | Gridded Ion Thruster, Wet Iodine propellant with valve [5]
- MarCo | Warm gas Thruster, Heated aluminum self-contained R-236fa storage [6]
- NEA-Scout | 86 sqft Solar Sail [7]

1.2.4 Standards and Requirements

1.2.4.1 Pressure Vessels

For a pressure vessel to be certified for use in space, or any aerospace vehicle, the system must pass a variety of safety requirements. These are of great importance due to the nature of a pressure vessel posing a potential explosive danger to personnel or launch vehicles and payload. The following requirements from AFSPCMAN91-710v3 [19] involve validating:

- Using industry/government standard process/procedures for manufacture
- Finite element or equivalent for Stress, Strain, Displacement

- Calculation of minimum margins of materials, weldments, and heat-affected zones
- Structure shall possess sufficient strength to withstand loads and MEOP in the expected operating conditions without detrimental deformation.
- Structure capable of withstanding ultimate external or internal loads and design burst pressure is in the expected operating environments or internal pressure without rupture.
- Margin of safety shall be positive and determined by analysis or testing at all expected critical temperatures.
- Shall possess adequate stiffness to preclude detrimental deformation at limit loads and pressures.
- Stiffness shall prevent all detrimental instabilities of coupled vibration modes, minimize loads and dynamic response associated with flexibility.
- Thermal effects, including heating rates, temperatures, thermal gradient, thermal stresses and deformations and physical and mechanical protein of material shall be considered.
- All pressurized structures shall be proof pressure tested to verify structural integrity.
- Proof fluids shall be compatible with tank materials.
- Accept/reject criteria shall be formulated before acceptance proof test.
- Testing shall include random vibration testing.

  ** All requirements above have been cited from AFSPCMAN91-710v3 [19]*

1.2.4.2 Launch Vehicles

The launch vehicle that will be used to meet the requirements will be the SpaceX Falcon 9. These requirements are given on a basis of Required, Advised, or Not Required for all of the important types of analyses which can be seen in table 1. The details for each type of analyses will undergo a more in-depth discussion in their corresponding results sections in the following chapters. Although the requirements state that Quasi Static and Sine Vibration are not required, analyses will still be conducted for proof of concept within this paper.

Table 1 Falcon 9 rideshare containerized CubeSat unit test levels and durations [24]

Test	Required/Advised	Qualification (Unit Not Flown)
Quasi Static Load	Not Required	
Sine Vibration		
Acoustic		
Shock	Advised	6 dB above MPE, 3 times in each of 3 orthogonal axes
Random Vibration	REQUIRED	3dB above acceptance for 2 minutes in each of 3 axes
Electromagnetic Compatibility	REQUIRED	6dB EMISM by Test or 12 dB EMISM by Analysis
Combined Thermal Vacuum and Thermal Cycle	Advised	±10°C beyond acceptance for 27 cycles total

Pressure Systems	REQUIRED	Pressures as specified in Table 6.3.12-2 of SMC-s-016 following acceptance proof pressure tests, duration sufficient to collect data. Minimum 2.0 times MEOP
System-Level Pressure Leak Test	REQUIRED	Not Required
Pressure Vessel Leak Test	REQUIRED	Not Required

1.2.5 Finite Element Analysis

1.2.5.1 Introduction to FEA

When designing components that will eventually become space certified, there are a bunch of requirements that need to be addressed beforehand. For example, the structure of a CubeSat must be able to withstand certain stresses and strain along with vibrational loads from the launch vehicle. To measure if the component meets certain requirements, a test must be conducted to ensure the system passes with a factor lesser than the maximum allowable value. Physically testing every iteration of every prototype can be very expensive and wasteful as the design will likely change often. In addition, there are many aspects of data within a part that cannot be measured due to geometry and physical limitations. With the help of powerful mathematical solvers that can be used on most computers, finite element analysis allows the designer to test certain parameters of a component without needing to manufacture it. Finite element works by taking complex 3D objects and dividing them into smaller elements (finite elements), each element has its own number of nodes or nodal points depending on its complexity [15]. This mesh of nodes is then numerically solved in terms of what the designer is trying to solve. Solvers can be used to find the stress/strain curves of a CubeSat structure, the harmonic frequency of the solar panels, or thermal expansion of the thruster nozzle. Finite element analysis can also be used to find parameters in 2D objects as well. The entire FEA process can be summed up and listed as three main groups.

- Preprocessing: Covers all boundary conditions, material selection, appliance, mesh generation and modification, surface smoothness, interaction, and frequency [15]
- Solution: Solver of unidentified numbers of the primary field of variables [15]
- Post Processing: Comprises of sophisticated routines utilized for further plotting graphs and illustrating results [15]

1.3 Project Objective

The goal of this project is to investigate methods into designing a conformal expulsion tank for the use in CubeSats. The tank will be tailored towards using the variety of available green monopropellants as the propellant. This process will involve designing multiple iterations of propellant tanks in which all will go through a series of static structural and modal FEA simulations. The data from these simulations will be compared with similar types of expulsion systems and held ultimately to all applicable safety standards and regulations.

1.4 Methodology

Trade studies will be performed to make a final decision on the type of expulsion system to be designed, either a Bladder, Diaphragm or Piston. The chosen system will then go through a design phase to give options about the most suitable design to proceed. This device will be designed in different size configurations, in reference to CubeSat size, to prove its modularity. Tests will be performed on every available option for the various CubeSat sizes. Static structural and modal analysis simulations will be performed on each configuration based on different materials needed for specific propellants. Static structural analysis will determine the max amount of stress and deformation the tank will go through until the max allowable pressure is achieved. This max allowable pressure will give an idea of what the safety factor of the tank should be. Modal vibration analysis will determine the natural frequencies of each configuration and determine possible failure points. A range of additional vibration analyses will be performed as necessary. With this data, tank configurations will be integrated into mock CubeSat variations of size reference to perform further analysis to measure how the structure affects performance/failures. Once a baseline set of data is achieved for every configuration, a few of the tanks will go through an optimization solver to decrease the overall mass while maintaining its strength. Additional optimization will investigate the use of lattice structures such as gyroids to decrease mass. Once a suitable design is made, all analyses will be performed and compared to the original design to identify the amount of weight savings that can be achieved.

2. System Design

2.1 Developing System Level Requirements

2.1.1 Requirements from Industry Standards

When designing a system to be used in the space environment, it is extremely important to ensure that the system design meets all of the standards needed to pass qualification tests for certification. Standards developed by industry committees, such as NASA or the Air Force, set guidelines so that safety is the number one aspect. These guidelines determine what standards must be met when creating the system requirements. System requirements are a set of values or conditions that must be met for the system to be successful. These requirements are often not a fixed value but instead are a range of values that the system must fall within. The following set of high-level system requirements has been created using the standards for pressure vessels listed in section 1.2.4:

- All manufactured or purchased hardware must use industry or government processes and procedures.
- All parts subject to pressure must be analyzed using Finite Element of equivalent for Stress, Strain, and Displacement.
- Structure shall possess sufficient strength to withstand MEOP loads of 750 psi without detrimental deformation.
- Structure shall be capable of withstanding ultimate internal loads and design burst pressure is within 1125 & 1650 psi.
- The margin of safety shall be between 1.5 & 2.2, determined by analysis and verified by proof/burst testing.
- Structure shall possess adequate strength to preclude detrimental deformation at limit pressures of 750 psi.
- Stiffness shall prevent all detrimental instabilities of coupled vibration modes determined by launch vehicle, minimize loads and the loads associated with flexibility.
- All hardware, mounting points, tolerances, and materials must consider thermal effects, gradients, temperatures, and stresses.
- Proof fluids must be compatible with tank materials.
- Accept/Reject Criteria shall be formulated before acceptance proof test.

2.1.2 Subsystem Requirements

In addition to the requirements set by industry standards, there is also a set of requirements driven by the needs, goals, and objectives of the mission itself including all of the individual components used. The objectives of this system involve:

- Develop a modular propellant delivery system suitable for CubeSats.
- Utilize as little volume and mass as possible.
- Store propellants, such as HTP, at an operational pressure of 750 psi.

- Use green monopropellants as the fuel/oxidizer source.
- Support a high enough propellant mass flow rate needed for a 1N thruster.
- Store enough propellant per unit of CubeSat payload to support a suitable mission lifespan.
- Develop a way to reduce pressure blowdown.

All of the system components will have at least one aspect that derives requirements for their subsystem. Listed below are the requirements for the structures subsystem, and the acceptance criteria for the full system.

2.1.2.1 Structures

The structures subsystem involves the tank design and materials chosen. The design and materials will dictate, based on the mission, what the requirements will be. The structures subsystem requirements are as follows:

- The tank must be made from materials compatible with HTP.
- The tank must combine both the pressurant and propellant into one tank.
- The tank design must be modular and suitable for use with 3U, 6U, and 12U CubeSats.
- The tank design must be able to support an operational pressure of 750 psi and burst pressure between 1125 and 1650 psi.
- Part interaction tolerances must be suitable for leakage prevention and dynamic movement as necessary.

2.1.2.2 Acceptance Criteria

When considering a set of design requirements, there will always naturally some amount of variation in the outcome or performance of a system. Because of this, acceptance criteria must be established to define what results will be accepted or rejected. Some of the critical performance variables and their acceptance criteria are as follows:

- Allowable maximum tank pressures can vary ±20 psi, Reject any pressure ±21 psi greater or lesser than 1125-1650 psi.
    - Any pressures above or below the 1125-1350 psi range will result in a safety factor lesser or greater than 1.5-2.2. A safety factor less than 1.5 means the tank will not meet safety standards, and above 2.2 suggests that the tank is overbuilt and likely has unnecessary mass.
- Allowable tank leakage can be a maximum of $1x10^{-6}$ cc/sec, Reject any leak rate higher.
    - Due to the oxidative properties of HTP, the leakage needs to be as close to zero as possible. Must be tested using NASA-STD-7012 Leak Test Requirements [16].
- Allowable propellant flow rate is dependent on thruster used.
    - Every thruster has its own nominal flow rate, an example 1N thruster requires a mass flow rate of 0.65 g/s
- Allowable blowdown must be at most a 4 to 1 ratio of propellant pressure at start, to the pressure at end-of-life cycle, Reject any ratio higher.

    - Blowdown is a natural expected behavior of a pressurized system. As the propellant is expelled, the volume of air increases, this causes the pressure to decrease. The pressure when the propellant is empty needs to be at least 1/4 of the starting pressure because, at lower pressures, there will not be sufficient pressure to feed the thruster.
- Allowable deformation must be within 1.18 & 1.23% at maximum operation pressure, Reject percentage higher.
    - Deformation of an aluminum propellant tank can cause the material to rupture causing a catastrophic failure. Deformation must be kept to a minimum to prevent failure.

2.2 Design Aspects

2.2.1 Piston Expulsion Device

For this system, the piston type expulsion tank was chosen to design and test. The piston type was chosen over bladder and diaphragm due to the ease of manufacturability of the parts needed. All of the parts can be designed in such a way to use simple, low-cost custom parts that any machine shop can produce. In addition, the parts can easily be designed to use off the shelf components and sealing materials. If given the opportunity, the tank itself could be reused many times by simply refilling the propellant. This could open up the possibility for in space refilling and reduce the waste from end-of-life satellites. A piston device offers scalability by being able to extend or shorten the body height of the tank which increases the overall volume of usable propellant. Another aspect that the piston device can offer is the ability to handle and operate at very high pressures. Although there are many advantages of using a piston device, it also comes with its own set of disadvantages as well. One of the biggest potential issues is the risk of caulking, or when the piston tilts slightly, which causes either the piston to get stuck, a propellant leak, or both. With this in mind, the design must have a stiff central guide rod to ensure the piston will slide straight and smoothly through the cylinder. The addition of a guide rod now introduces another area that needs sealing and a possible area that could leak. Due to the need to seal between the piston and guide rod, and the piston and cylinder wall, gaps in these areas must be held to a tight tolerance to prevent leakage but also allow for movement.

2.2.2 Rectangular Design

When designing a pressure vessel, generally designers would pick the use of a cylindrical or spherical structure due to its natural high strength capabilities. There is nothing wrong with using that design, but in most cases, it requires the propellant to be stored in a separate tank than the pressurant. The pressurant is used to drive the expulsion device and, because it is stored in a separate tank, the payload must provide more volume for the expulsion system. As an objective to reduce the overall weight needed for a CubeSat expulsion system, the clear solution is to combine the two tanks into one device. Since CubeSats are, as the name states, cubes, the way to utilize the most use from the volume is to fill the space with an additional cube or rectangle. Consequently, the solution to this objective involves using a rectangular tank. This can be visualized by drawing a rectangle that is 95 mm wide, 95 mm deep, and 180 mm tall. On the face

of the 95 x 95 mm square, a circle is drawn exactly at the center with a diameter of 90 mm. Draw another circle at the same center as the first, but with a diameter of 86mm. Extrude subtract the volume of only the second circle through the length of the rectangle which creates a cylinder of 86 mm diameter with a length of 180 mm. Referencing the same face as the pervious step, draw an additional square from the same center point, with a distance of 4 mm between the edges of the new square to the edges of the 95mm square. Using the new square and the 90 mm circle, four triangles are created in each of the corners of the 95 mm square where the new square and the 90 mm circle intersect. Extrude subtract each of these four triangles through the 180 mm length and now there is the cylinder with four triangular volumes around it. Filets of 1/8" radius must be added to each of the triangular corners to allow for manufacturability and a bonus of added strength. A top view showing the details of the cuts can be seen in figure 2.1. Not only does this design save weight by removing one of the two tanks, but it also decreases the amount of volume required to achieve the same result. With less mass and more available volume, the tank volume can be further increased to hold more propellant. The volume of the cylinder below the piston is where the propellant will be stored and is sealed from the volume above the piston. In each of the corner pockets is where the pressurant will be stored, which is connected to the volume above the piston.

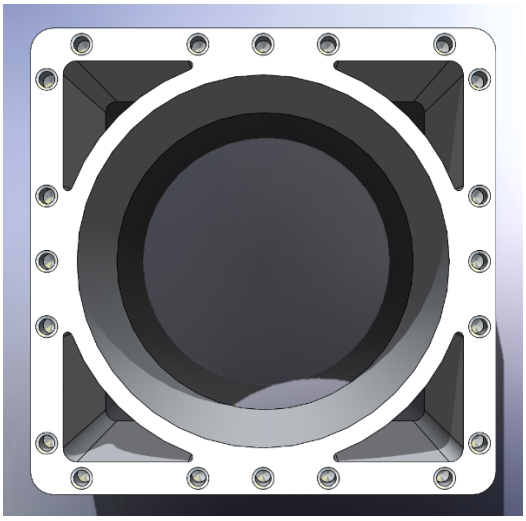

Figure 2.1 Top view of rectangular tank with cutout cylinder and corner pockets

2.2.2.1 Top & Bottom Plates

Since the system needs to be sealed to be able to hold any contents, a top and bottom plate must be made to close the system. These plates must house the necessary channels for the delivery of propellant or pressurant. They must also contain a seal that prevents either propellant or pressurant from escaping out of the side of the tank or leaking internally. An important point of having a separate top and bottom plate is that they can be removed for ease of assembly or inspection. Additionally, they can be replaced when new design updates are made, without the need to remake the entire tank.

Each of the plates has their own special features that ensure proper function of the system. The top plate has channels drilled through from one side to the other and will be placed so that they

intersect through the corner pockets. These points of intersection allow for the pressurant gas to maintain equal pressure between each of the corners and are what connects the corners to the upper side of the cylinder. An example of the top plate can be seen in figure 2.2, where the closest surface was made transparent to show the details of the internal channels. The bottom plate also has channels drilled into it, but they do not go all the way through, they stop about half way through so that the drain holes can be drilled towards the center of the plate. Another feature of the bottom plate is that it involves using an angled profile cut to guide the propellant towards the drain holes as it is being compressed. An example of the bottom plate can be seen in figure 2.3, where the closest face was made transparent to show internal details of the channels. After drilling the channels in the plates, a few holes now have the ability to vent to the outside. This can be taken advantage of by allowing the use of pressure fittings for either propellant filling or delivery to the thruster. Specifically, the top plate will have a pressurant feed line, and the bottom will have a propellant exit fitting to the thruster. These only use one of the four drilled holes in each of the plates, so a threaded plug with sealant must be used to seal the tank.

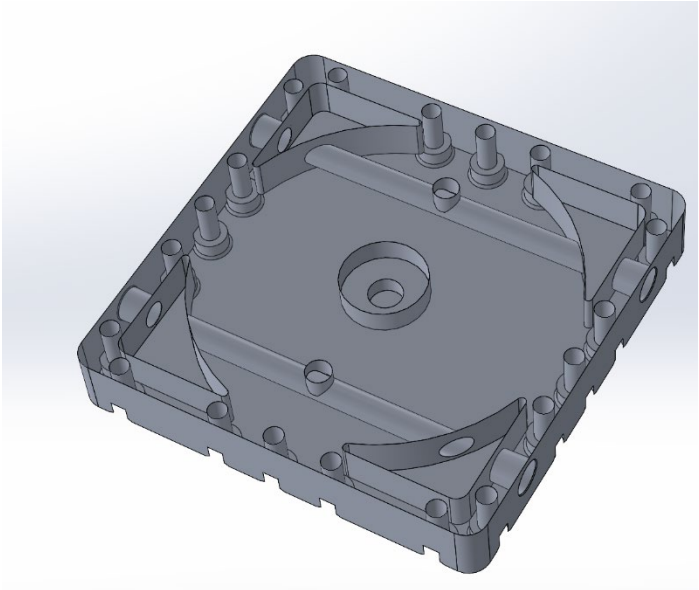

Figure 2.2 Top plate with upper face transparent to show inner channels

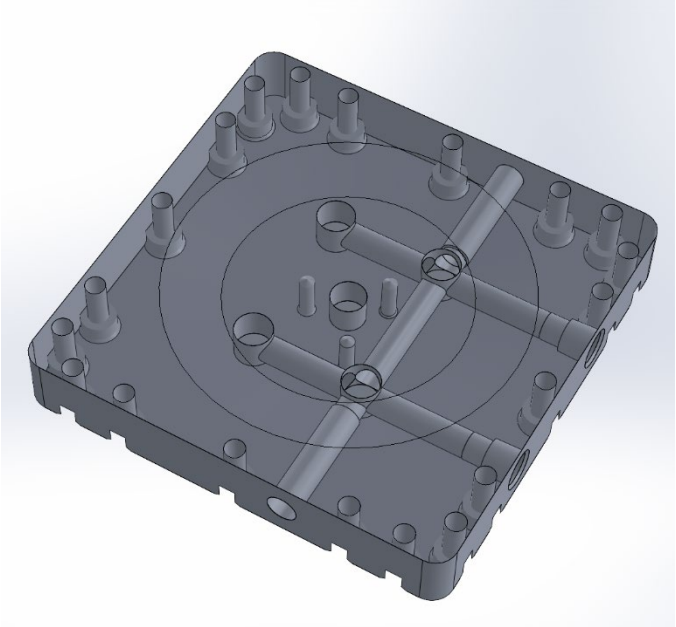

Figure 2.3 Bottom plate with upper face transparent to show inner channels

When looking into the sealing capabilities of a gasket compressed between two flat plates, a simple equation can be used to calculate the force required to compress a gasket at a certain torque. This is done by just dividing the torque applied by the area of the plate. With these plates both having an approximate area of 15.5 in^2, ignoring all of the necessary hole cutouts, to torque the plate at 60 in.lb, a force of 930 lb/in must be applied. This force can be reduced by decreasing the area needing to be compressed. A solution to this is to add ridges along of the sealing perimeters around each of the corners and the cylinder. To do this, a small 1 mm by 1 mm ridge with a small chamfer, to prevent sharp edges, was added. This new area was reduced to only 0.861 in^2, which decreased the needed force to 69.7 lb/in. These ridges that were added to the plates can be seen in figure 2.4. The bolt pattern and number of bolts were chosen to miss the drilled channels and include as many fasteners as possible. This gave a total of 20 bolts per plate.

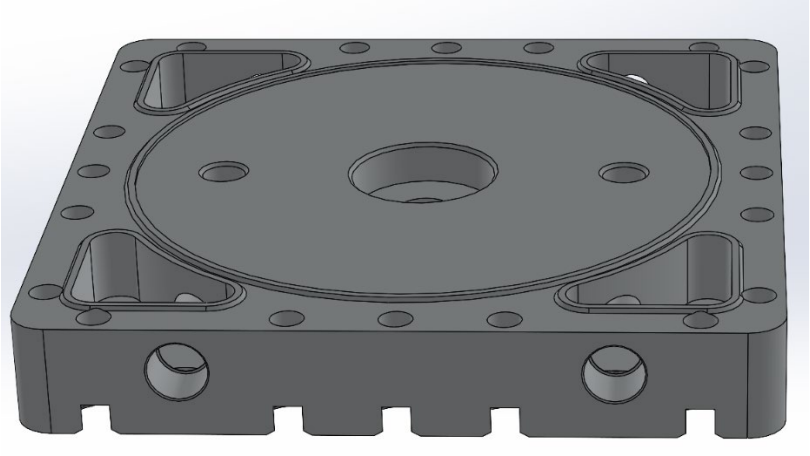

Figure 2.4 Top plate with the added ridges to reduce amount of applied torque

2.2.2.2 Piston Design

Possibly one of the most important parts of a piston expulsion system is the piston itself. It must contain characteristics of high stiffness, but also to retain its dynamic capabilities. Additionally, the piston must remain straight for the entire length of the cylinder to prevent wedging itself stuck in the cylinder due to caulking. The piston must also hold true a very tight tolerance between the outer diameter of the piston and the cylinder wall to prevent either propellant or pressurant from leaking past. Between each of the mating surfaces of the guide and cylinder wall to the piston must contain rubber seals to achieve zero leakage.

A common mistake that could cause the system to initially seal but fail once the piston starts to move is the use of an O-Ring. In this situation, since the system is dynamic, X-rings must be used in place of the O-rings because O-rings are known to roll in dynamic situations which would cause a leak. X-rings, due to their geometry, prevent any kind of rolling and ensure the dynamic system will remain sealed as the piston moves. Using just one X-ring between the mating surfaces would possibly be sufficient enough, but for redundancy, two X-rings will be placed between each mating surface in case one fails during its use. To seal between the piston and the cylinder wall, two guide channels dimensioned to the proper width to fit the X-ring will be cut in the outer diameter of the piston. The cut edges of the piston are also required to be chamfered or smoothed to prevent any sharp edges that would cut the gasket during installation or use.

For the guide rod to be most effective, a single rod needs to be placed directly through the center of the piston. To further prevent caulking, the area in contact with the guide rod was also lengthened. Similar to the outer diameter seals, the inner bore of the piston must also contain two X-rings for redundant sealing. This involved cutting the dimension of the proper width of the X-rings into the bore of the inner hole in two places. One was placed towards the top of the piston and another towards the bottom. The area between these two X-rings needed to be polished mirror smooth to ensure smooth sliding along the guide rod since they would constantly be in contact. An example section view of the piston showing the details of the X-ring channels can be seen in figure 2.5. To promote a high amount of stiffness, stronger materials that are different than the body will be used. Referring back to the bottom plate and its angled profiles, the piston must also match the same profile to ensure the most propellant transfer from the tank.

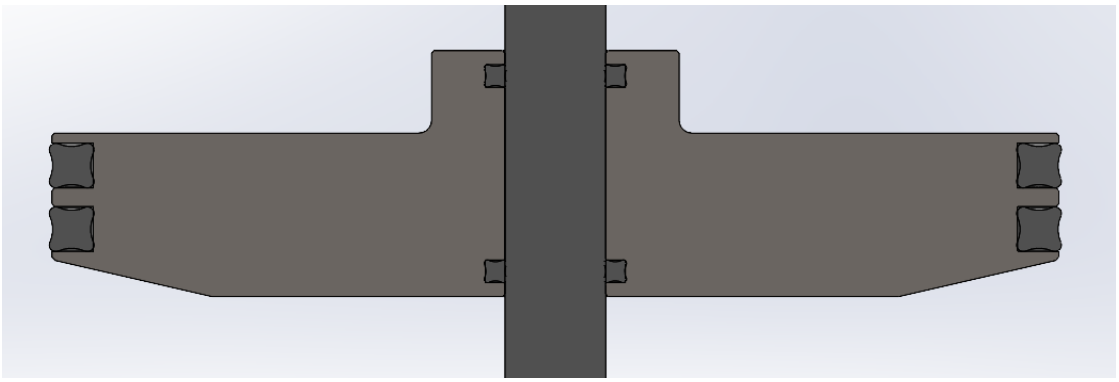

Figure 2.5 Section view of the piston to reveal X-ring channel details

2.2.2.3 Types of Hardware and Materials

Since the design of this system uses multiple removable parts, they need a way to be fastened together while maintaining comparable strength properties as if it was a single part. As stated in section 2.2.2.1, the top and bottom plates will use 20 bolts per plate to fasten to the body of the tank. The bolts have been chosen to be an M3 x 0.5 hex socket cap, with a length of 1 inch. These bolts are actually very small in thread diameter, so to counter this, black oxide bolts will be used due to their very high strength compared to any other material available. Using black oxide bolts does not need to worry about being compatible with the propellants, because they will never be in contact during expected use. That said, any surface or component that is in contact with the propellant must be compatible. With the monopropellant HTP in mind, there are very few materials that are compatible due to HTP being a very good oxidizer. Two metals that are compatible with HTP are 6061 aluminum and 316L Stainless Steel (SS). Technically, 316L SS is slightly susceptible to the oxidation of HTP, so it must be passivated first using 30% hydrogen peroxide before it can be in contact with the 90% concentration. Passivation ensures that the surface of the 316 SS component will have an oxidation layer which protects the surface from further oxidation or damage.

For the construction of the tank, the body and both of the top and bottom plates will be made from 6061-T6 aluminum. The piston and guide rod will both be made from 316L SS. In addition to the tank components, all of the fittings, solenoids, tubing, and manifolds must also be made from either 6061 aluminum or 316L SS. Most of the components will be found available in 316L SS due its high strength capabilities. Metals are not the only materials susceptible to the oxidization from HTP, compatible rubbers used for the seals must also be selected. The list of compatible rubbers is also short which contain Viton and PTFE, also known as Teflon. Viton will be used for the main gaskets between the top and bottom plates and the body. The available sheet stock that was chosen has a 1/16” thickness and hardness durometer of 75A. This sheet stock is not the only thing that needs to be made from Viton, the X-rings for the piston, and the seals inside every solenoid or relief valve must also be made from Viton.

2.2.2.4 Types of Holes

From section 2.2.2.1, it was said that the drilled holes in the side of the plates will either be used for fluid delivery fittings, or simply plugged to seal the system. To be able to properly install these fittings or plugs, a set of threads must be cut into the drilled holes which match the threads on the fitting or plug. Not all thread types are the same so it is worth mentioning the different types that will be considered for use in the system. A very common thread type usually found on pipes is called NPT threads, which are tapered from small diameter to larger diameter from the edge of the pipe. NPT threads are supposed to be able to self-seal without the need for gaskets or sealant, but often times still require a thread sealant tape such as PTFE. This has the advantage of being found on almost every type of fitting available. Some disadvantages of NPT threads are that they will leak if not properly torqued or sealed, it is hard to model the proper depth at which they will be fully seated, and they need special taps or dies to cut the threads. The other thread type that will be considered is the standard straight threads, but with the addition of a sealing ring. This sealing ring could be an aluminum ring that crushes when tightened, or a rubber O-ring likely made from Viton. Straight threads do not need special taps or dies, they are easy to create threads, and the hole depth is only limited to the length of the tool. The holes used to fasten the plate to the body will use a straight threads that uses a bottoming tap that can cut threads into a hole with a bottom.

2.2.2.5 Fluid Handling

Since this is a propellant tank that will hold fluids, details about fluid flow will need to be discussed. One of the most important variables to the entire system is the mass flow rate of the propellant to the thruster. This depends on a few different aspects such as the required intake of the thruster, the inner diameter of the tubing between the tank and thruster, and the pressure available in the tank. For a 1N monopropellant thruster, it can be assumed to require an intake of 0.65 g/s of HTP. If the system holds 1 L of HTP, the thruster can be estimated to have about 1,538 seconds of usable propellant. The potential tubing used for the system has not only a variety of inner and outer diameters, but also wall thicknesses. Outer diameters of 1/16” or less will not be considered due to their high risk of collapsing while being bent to shape. The diameters of 1/8” and 1/4” will be most suitable for this application. They will be made from 316L SS, where the 1/8” diameter will be used to connect the tank to the various manifolds and solenoids, and the 1/4” will be used for filling the tank.

To control the flow of the propellant, solenoids must be used to start and stop the flow. These must be able to withstand the high pressures of the propellant and also be able to operate above maximum tank pressure. As stated in section 2.2.2.3, the solenoids will be chosen to be made from 316L SS and must contain a seal made from Viton. Similar to solenoids, the system must include safety pressure relief valves. These are set in line with both the pressurant and propellant delivery channels and ensure the system can never reach its maximum burst pressure. This is done with the use of specially calibrated springs or valves that will either blow out, or spring open when a specific set pressure is reached. Since the target operational pressure is 750 psi and the burst pressure will be designed to be 1125-1350 psi, the pressure relief valve selected will have a set relief pressure of 900 psi.

Another important component to the fluid system is the use of a pressure transducer which is able to measure the available pressure in the tank. Pressure transducers could be used on each of the pressurant and propellant sides to measure their pressures individually, even though they are expected to be equal. This could be useful in diagnosing the system in the case of a caulked stuck piston, which could be identified by unequal pressures.

2.2.2.6 Integration into CubeSats

Overall, this propellant system is designed to be integrated into a CubeSat structure, which means the dimensions of the system must be defined to ensure proper integration. Since CubeSats are restricted to a depth of exactly 10 cm, with some of this taken by the thickness of structure material, the width and depth dimensions of the tank must be limited to 95 mm. The tank will be set at 95 mm width and depth, but the length will depend on the size of CubeSat it will be integrating with. For a 3U CubeSat, the length will be limited to 10 cm so that there is still enough payload volume for science experiments. 6U and 12U sized tanks can be between 20 cm and 30 cm since there is more space available and will generally need more propellant for their missions. With the standard mass of CubeSats being 2.2 kg per U, the system must remain light enough to not take too much mass away from the rest of the CubeSat. Another aspect that needs to be addressed for integration is the mounting points of the tank to the CubeSat. This will need to be chosen after completing a series of trials using FEA to provide the best strength and the least negative effect on vibrational harmonics. Various mounting positions involving either the plates or tank body will be considered, as well as its orientation.

2.3 Simulation Planning

2.3.1 Static Structural

Once a system has been fully designed and modeled in CAD software, the system must be tested to ensure it meets the pressure requirements set in section 2.1.2.1. Manufacturing a tank every time a test is performed will prove to be extremely costly, and unnecessary. This does not mean that a prototype model never needs to be manufactured at all, proof and burst certification must still be performed on an actual tank. The CAD model can initially be tested using FEA software, such as Ansys, to perform a static structure simulation to find a solution that is worth manufacturing. Static structural can calculate a high-fidelity approximation of all the internal stresses, strain, or displacements that the system will experience under a defined load. This is very important because it will not only highlight areas of highest stress and displacement, but also provide an assumption of what the burst pressure of the tank could be. The burst pressure is determined by examining the maximum stress value at the point it surpasses the Von Mises yield strength of the material. It is at this time when the material will be assumed to fracture. To calculate the analytical safety factor, the pressure of expected fracture is then divided by the maximum operational pressure which is required to give a value between 1.5 and 1.8. For the analysis to give an accurate result, the model must include as much detail as possible such as modeling the hardware and their torque values. Analysis will need to be done on every configuration of the system and their different sizes or materials. Once analysis agrees with the

requirements, a prototype test tank can be manufactured to undergo a series of proof, and a final burst test to validate the simulation analysis and certify the system.

2.3.2 Vibrational Analysis

Vibrational analysis can be conducted as either a preliminary system checks before conducting static analysis or can be done after static analysis to first ensure the system geometry will pass the initial structural requirements. In this project, the analysis will start by conducting modal analysis to find the natural frequencies. This is very important because launch vehicles will always produce some value of vibrational harmonics that the payload must be able to survive. An issue developed from vibrations is that it can cause fasteners to loosen and either rotate out or detach from their mounting points. Additionally, it can cause the system to oscillate at a certain frequency which could permanently damage a component or the entire system from the material displacement. The system will be put through a sweep of vibration frequencies, random frequencies, and the specific frequencies defined in the launch vehicle interface document. Resultant components that do not meet the vibrational requirements will need to be fixed with a redesign and updated static structural analysis.

2.3.3 CFD Fluid Flow

Once the systems have passed the static structural and vibrational analysis, the system will be modeled in CFD to simulate the fluid flow through the system. This is important to verify how the system performs and is key for testing what size inner diameter tubing is needed to meet the necessary mass flow rate. CFD can also identify any areas of back pressure, stagnant pockets of propellant, or areas where the propellant becomes too turbulent. The goal of the propellant outflow is to be as smooth and least resistant as possible to avoid any fluctuations of mass flow rate. If a major issue with the mass flow rate is found, the design must be fixed and retested through static and vibrational analysis. Ideally, the system should pass all the requirements of static structural, vibrational, and CFD analyses in simulation before the system is manufactured and subject to real equivalent tests.

3. Finite Elements

3.1 Background

The finite element method (FEM), as stated in section 1.2.5.1, is a computational tool that uses powerful mathematical solvers to predict the stresses, strains, displacements that a complex geometry might experience in defined scenarios. The FEM process involves discretizing partial differential equations (PDE) to obtain algebraic equations to approximate their solutions of the elements within the structure. There are some cases where ordinary differential equations (ODE), with respect to time, are left over with the algebraic equations. An example of discretizing a 2D structure can be seen in figure 3.1. These elements connect with the use of nodes, which are defined points in space that have defined degrees of freedom. When the continuum system is split into elements, these elements each represent a single cell that collectively represents the entire geometry in the form of a mesh. The node cells can be made of basic shapes such as a triangle or square for 2D cases, and tetrahedral or brick for 3D cases. The number of nodes per cell is dependent on the fidelity of the solver used in the analysis, with more nodes will usually result in higher accuracy for curved edges. This, however, does not mean that decreasing the size of the cell to the smallest possible will result in exact calculations of the resultant. There is a point where increasing the number of nodes will plateau at an increased accuracy, but still will not be an exact solution since FEM is an approximation.

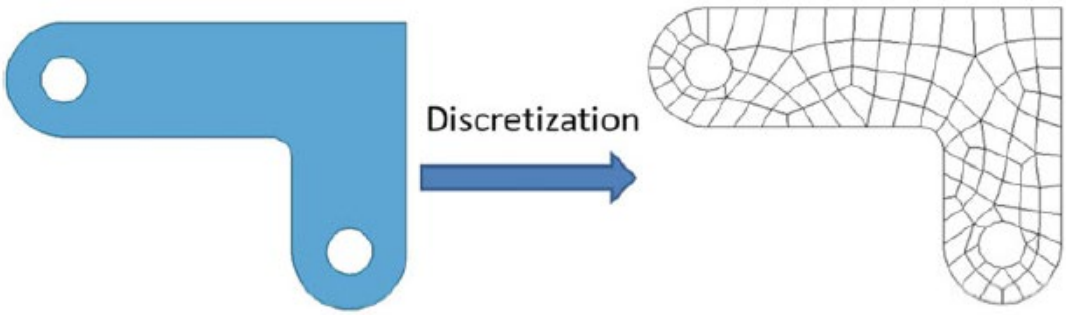

Figure 3.1 Finite element discretization of a 2D structure [17]

3.2 Theory of Elasticity

When a geometry of solid material is slightly deformed from an external force, the internal properties of elasticity will allow the material to return to its original state, assuming it was not permanently deformed. An external force applied to a specified area is known as stress, while the amount of deformation is called the strain [22]. For this project, the models will undergo the assumption that the materials that deform from an external force will return to their original shape.

The goal will be to test the model through a variety of scenarios so that internal stresses or strains that could cause the part to fail will be identified. These scenarios include static structural, and vibrational (dynamic) analysis. To do this, mathematical models will need to be identified along with the assumptions that will be made. Following the mathematical models is the numerical solution procedure, or the strategy to find the solution along with the errors that arise from this strategy. With these mathematical models and solution procedures, the geometry will be defined to create a mesh and finish the model setup. With this in place, the solution and results can be found and finally verified and validated.

3.2.1 Assumptions

Due to the complexity of the finite element calculations, a few basic assumptions will be set in place to make solving the problems feasible for this project. The application of these assumptions depends on the finite element solver, some of the high-cost software programs can solve higher complexity problems while not making the assumptions that will be listed in this section. The assumptions in this section are to be used to simplify the computational load that the solvers will face. The four basic assumptions are as follows.

3.2.1.1 Continuum

For the continuum, the assumption is made that matter in the body of material is continuously distributed and fills the entire region of space it occupies [17]. This is advantageous because continuous functions are used to identify physics properties of stress and strain. This assumption only represents continuum on a macro scale, this is because anything less cannot be solved using finite element due to being discrete. This does not mean that the body needs to be solid throughout, where there are holes or empty spaces, the elements will treat them as a wall and only fill where there is material. For this project, the body will be continuous from element to element and will not have elements where there are holes or empty spaces.

3.2.1.2 Linear elasticity

Linear elasticity is a common assumption with material mechanical properties. Materials can have either linear or nonlinear mechanical properties. For nonlinear materials, the stress is nonlinearly changing with the strain since the start of stretch/compression, and for linear, the stress goes through a linear strain then changes to nonlinear after the yield point [17]. Most FEA software packages, especially Abaqus and LS-Dyna, are able to solve both linear and some sort of non-linear properties in materials. An example of a linear material changing to nonlinear can be seen in figure 3.2. The linear part is the rise over run, and changes to nonlinear after the yield strength point. Knowing the stress/strain curve of a material is very important because it gives information on other characteristics such as Young's modulus and more. The assumption of linear elasticity will be made for this project to allow for simple identification of material mechanical properties.

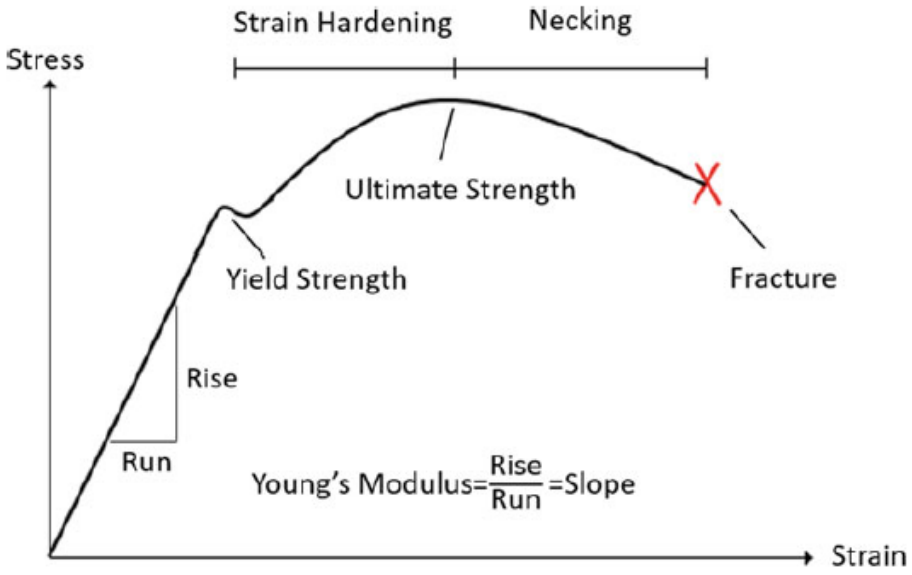

Figure 3.2 The stress/strain curve of a ductile material [17]

3.2.1.3 Isotropy and homogeneity

When a single material represents the same mechanical property anywhere in the body and in all possible directions, the material is considered isotropic and homogenous. The other classification is when there are multiple materials involved and a material contains fiber reinforcement which is then considered anisotropic and heterogenous. While all FEM solvers can solve for isotropic and homogenous materials, there are software packages which can solve for composite materials which are anisotropic and are generally heterogenous. For this project, the assumption of isotropic and homogenous materials will be used ultimately for simplifying the complexity of the calculations. The materials used will be considered consistent through each part, so that the assumption can be made to have no variation in mechanical properties throughout the material.

3.2.1.4 Small deformation

The last assumption, in part with linear elasticity, will be that the material body will only experience a deformation and displacement that is very small. This is good because the small deformations of the body can be ignored and consequently the high order parts of the Taylor series equation can be ignored, and subsequent equations simplified to linear elastic equations [17]. There are solvers that can handle large displacements which updates the stiffness as the load changes in steps.

3.2.2 Equations for the Theory of Elasticity

Whether the solver is solving a 2D or 3D case, there are mathematical equations set in place to solve these geometries. These equations are complex forms of simple physics equations, and similar to any other physics problems, the first step of the solution is to define the equations of motion. Each of the solvers use the same fundamental equation but with specific variables either constant, absent, or as a function of time. This equation is:

$$[M]\{\ddot{u}\} + [C]\{\dot{u}\} + [K]\{u\} = \{F(t)\} \tag{3.1}$$

Where [23]:

- [M] is the mass matrix
- [C] is the damping matrix
- [K] is the stiffness matrix
- $\{\ddot{u}\}$ is the resultant acceleration vector
- $\{\dot{u}\}$ is the velocity
- $\{u\}$ is the displacement vector
- $F(t)$ is the forcing function vector in time

3.2.2.1 Equilibrium Equation

For structural vibration, the system will be treated as a system in dynamic equilibrium in relation to static equilibrium. This will allow for the equations of motion to be written with relation to Newton's second law of motion. Newton's second law states that "the rate of change of momentum of a mass is equal to the force acting on it" [18]. Figure 3.3 shows a 2D plane problem which indicates that the sum of all forces in x, y, and any moments must equal zero.

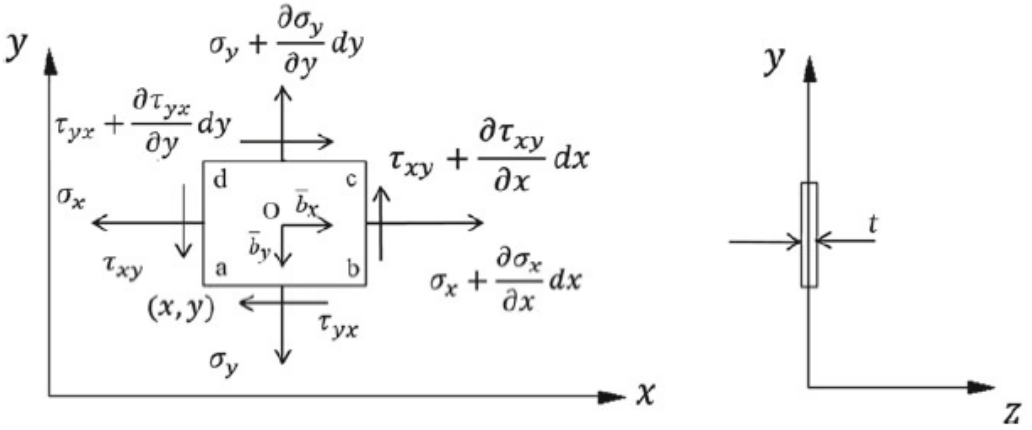

Figure 3.3 A representative 2D unit under the balanced forces [17]

For a 2D plane problem, the equilibrium equations are:

$$\begin{gathered}\frac{\partial \sigma_x}{\partial x}+\frac{\partial \tau_{yx}}{\partial y}+\bar{b}_x=0 \\ \frac{\partial \sigma_y}{\partial y}+\frac{\partial \tau_{xy}}{\partial x}+\bar{b}_y=0 \\ \tau_{xy}=\tau_{yx}\end{gathered} \tag{3.2}$$

For 3D problems, the equilibrium equations are:

$$\begin{cases}\dfrac{\partial \sigma_x}{\partial x}+\dfrac{\partial \tau_{yx}}{\partial y}+\dfrac{\partial \tau_{zx}}{\partial z}+b_x=0 \\ \dfrac{\partial \tau_{xy}}{\partial x}+\dfrac{\partial \sigma_y}{\partial y}+\dfrac{\partial \tau_{zy}}{\partial z}+b_y=0 \\ \dfrac{\partial \tau_{xz}}{\partial x}+\dfrac{\partial \tau_{yz}}{\partial y}+\dfrac{\partial \sigma_z}{\partial z}+b_z=0 \\ \tau_{xy}=\tau_{yx}, \tau_{xz}=\tau_{zx}, \tau_{zy}=\tau_{yz}\end{cases} \tag{3.3}$$

3.2.2.2 Strain-displacement equation

With complex geometries, adding the forces at each point in all directions can be challenging, using small deformation strain-displacements helps simplify the calculation. This relationship is referred to as the geometric equation and also the principle of displacements. The principle of virtual displacements states that 'if a system, which is in equilibrium under the action of a set of forces, is subjected to a virtual displacement, then the work done by the forces will be zero' [18]. Figure 3.4, a 2D strain-displacement relationship, will be used to define the strain-displacement equations.

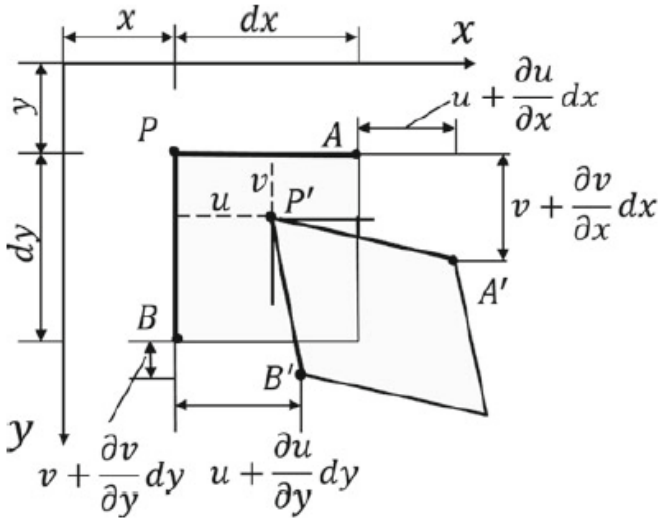

Figure 3.4 The diagram for deriving the strain formulation [17]

Since this is a 2D case and the assumption of small deformation is being made, the high order terms of the Taylor series can be ignored. The following equations show the displacements relation for 2D

$$\begin{aligned} \epsilon_x &= \frac{du}{dx} \\ \epsilon_y &= \frac{dv}{dx} \\ \gamma_{xy} &= \frac{\partial u}{\partial y} + \frac{\partial v}{\partial x} \end{aligned} \tag{3.4}$$

The 3D case for strain-displacement is

$$\epsilon_x = \frac{\partial u}{\partial x}, \epsilon_y = \frac{\partial v}{\partial y}, \epsilon_z = \frac{\partial w}{\partial z} \tag{3.5a}$$

$$\gamma_{xy} = \frac{\partial v}{\partial x} + \frac{\partial u}{\partial y}, \gamma_{yz} = \frac{\partial w}{\partial y} + \frac{\partial v}{\partial z}, \gamma_{zx} = \frac{\partial u}{\partial z} + \frac{\partial w}{\partial x} \tag{3.5b}$$

3.2.2.3 Stress-strain equation

Stress-strain relations, also called the constitutive relation or the physical relation, is where the physical variable such as Young's modulus are involved [17]. Since the assumption was made to have the materials as isotropic, linear elastic, and homogenous, their behavior can be described using only two variables. These two variables are Poisson's ratio and elastic modulus. Based on this assumption, the stress-strain equations are:

$$\begin{aligned} \sigma_x &= \frac{E(1-\mu)}{(1+\mu)(1-2\mu)}\left(\epsilon_x + \frac{\mu}{1-\mu}\epsilon_y + \frac{\mu}{1-\mu}\epsilon_z\right) \\ \sigma_y &= \frac{E(1-\mu)}{(1+\mu)(1-2\mu)}\left(\epsilon_y + \frac{\mu}{1-\mu}\epsilon_x + \frac{\mu}{1-\mu}\epsilon_z\right) \\ \sigma_z &= \frac{E(1-\mu)}{(1+\mu)(1-2\mu)}\left(\epsilon_z + \frac{\mu}{1-\mu}\epsilon_y + \frac{\mu}{1-\mu}\epsilon_x\right) \end{aligned} \tag{3.6a}$$

$$\begin{aligned} \tau_{xy} &= \frac{E}{2(1+\mu)}\gamma_{xy} \\ \tau_{yz} &= \frac{E}{2(1+\mu)}\gamma_{yz} \\ \tau_{zx} &= \frac{E}{2(1+\mu)}\gamma_{zx} \end{aligned} \tag{3.6b}$$

Relating back to the fundamental equation 3.1, the stress-strain relation results in a static linear problem where [C] = 0, [M] = 0, and [K] & $\{F(t)\}$ are constants. The resulting problem is the stiffness multiplied by displacement is equal to the force from the loads applied:

$$Ku = F \tag{3.7}$$

3.2.2.4 Form Correction

To properly set up the equations into the correct form for vibrational analysis, the strain-displacement, and stress-strain equations, 3.5 and 3.6, need to be combined. The PDE's need to be in this form so that they can be discretized into integrals and then algebraic equations. The combined equations are:

$$\begin{aligned}
\sigma_x &= \frac{E(1-\mu)}{(1+\mu)(1-2\mu)}\left(\frac{\partial u}{\partial x}+\frac{\mu}{1-\mu}\left(\frac{\partial v}{\partial y}\right)+\frac{\mu}{1-\mu}\left(\frac{\partial w}{\partial z}\right)\right)\\
\sigma_y &= \frac{E(1-\mu)}{(1+\mu)(1-2\mu)}\left(\frac{\partial v}{\partial y}+\frac{\mu}{1-\mu}\left(\frac{\partial u}{\partial x}\right)+\frac{\mu}{1-\mu}\left(\frac{\partial w}{\partial z}\right)\right) \qquad (3.8a)\\
\sigma_z &= \frac{E(1-\mu)}{(1+\mu)(1-2\mu)}\left(\frac{\partial w}{\partial z}+\frac{\mu}{1-\mu}\left(\frac{\partial v}{\partial y}\right)+\frac{\mu}{1-\mu}\left(\frac{\partial u}{\partial x}\right)\right)
\end{aligned}$$

$$\begin{aligned}
\tau_{xy} &= \frac{E}{2(1+\mu)}\left(\frac{\partial v}{\partial x}+\frac{\partial u}{\partial y}\right)\\
\tau_{yz} &= \frac{E}{2(1+\mu)}\left(\frac{\partial w}{\partial y}+\frac{\partial v}{\partial z}\right) \qquad (3.8b)\\
\tau_{zx} &= \frac{E}{2(1+\mu)}\left(\frac{\partial u}{\partial z}+\frac{\partial w}{\partial x}\right)
\end{aligned}$$

3.2.3 Boundary Conditions

An important step in the process of setting up a finite element analysis for a part is the definition of boundary conditions. Without boundary conditions, a part would not be able to display any movement because the boundaries are not defined. Displacement and force boundary conditions are two types of conditions, but only force boundary will be discussed. The forced boundary condition refers to regions of the deformable body where an external force applied to the boundary is defined [17]. In figure 3.5, S_p is this external force and shows the reactionary forces to keep the system in equilibrium.

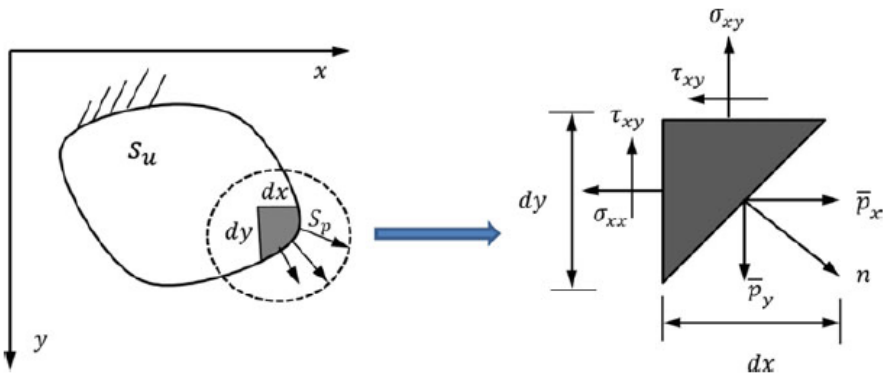

Figure 3.5 Illustration of the force boundary condition [17]

An issue that could arise when setting up boundary conditions is when there is a singularity. A singularity can occur when an external or internal force is directed to a single node. These can be identified where there is a single point that results in infinite stress. This is because the stress is equal to the force divided by the area. To make the problem non-singular, the determinant of the stiffness matrix [K] must not equal zero.

3.3 Structural Analysis

Finite element analysis, both static and dynamic, will be performed on the expulsion device to find as many, if any, failure points that might occur and their conditions of how it was able to fail. Static analysis primarily tests the systems stress, strain, and displacement characteristics in reaction to a defined load. It is important to test as many variables as possible within the expected work environment all the way until failure. This includes testing mounting point loads, pressure loads, and any static loads from manufacturing, transport, or the launch vehicle. Dynamic loads of interest are vibrational stresses, strains, and displacements. For aerospace applications, vibrational loads and acoustic noise are a huge design factor because they can cause unrepairable damage to structures and components. Vibrational loads and acoustic noise are practically unavoidable, so it is best for the designer to figure out ways to mitigate the risk of damage as much as possible. This section will discuss the different types of analyses with a more in-depth explanation of the vibrational analyses.

3.3.1 Static Analysis

For this expulsion device, the most critical quasi-static load is the operational and maximum pressure loads of the pressurant/propellant system. The second most critical dynamic load is the vibrational loads experienced from the launch vehicle.

Static structural analysis calculates the effects of steady state loading conditions on a structure, while ignoring inertia and damping effects caused by time-varying loads [19]. Static loads can include time-varying loads if they are approximated to be a static load that is equivalent. Addition loads include rotational velocity and gravity since they are steady. Although the

equations generated in section 3.2 are assumed to use linear elasticity, static structural can be either linear or nonlinear. As stated in section 3.2.2.3, this is a static linear problem where [C] = 0, [M] = 0, and [K] & $\{F(t)\}$ are constants resulting in equation 3.7. The function $\{F(t)\}$ is where all of the loads are contained. The types of loading that can be applied in a static analysis include [19]:

- Externally applied forces and pressures
- Steady-state inertial forces (such as gravity or rotational velocity)
- Imposed (nonzero) displacements
- Temperatures (for thermal strain)

3.3.2 Vibrational (Dynamic) Analysis

Vibrational analysis is very important to the success of any structure or component whether it will be used in space or on ground. Vibrations can be caused by many sources such as rocket engines, electric motors spinning, and sound waves. While many vibrations may not pose any immediate threat to the structural integrity of a system, it is crucial to find frequencies that can cause a risk of failure. Not all vibrations are the same and they are divided into sub-categories such as free vs. forced vibration, and sinusoidal vs. random vibration [20]. In addition to the different types of vibrations, there are also different types of analyses to detect and test for those types of vibrations. This section will discuss the types of vibrations and their analyses.

3.3.2.1 Free vs. Forced Vibrations

Free vibrations can be thought of as the natural response of how a part or structure will respond to a disturbance based on the part's mechanical properties. Knowing the mechanical properties of the material will allow the ability to predict how it will react. An example can be seen by when you strike a tuning fork that was tuned for 440 Hz, no matter how you strike the fork it will always produce a frequency of 440 Hz. Forced vibrations are the response of a structure when it is attached to something else that has a continuous force function. Depending on how the structure is constructed will determine the response to the force function. An example can be seen when examining a lawn mower, the motor will produce a continuous force function and how the handle is constructed will determine its response to the force function.

In Free and Forced vibrations, when referring back to equation 3.1, the forcing function $\{F(t)\}$ is equal to zero. The assumption of no damping, [C] = 0, was also made and with [M] and [K] constant the result is an Eigen value problem.

3.3.2.2 Modal Analysis

The most commonly used type of analysis is modal analysis due to its ability to identify natural frequencies, but also because it is needed to supplement the other types of analysis. That being said, modal analysis is can be used to find the natural frequencies of the structure and its mounting structures as well as identifying the mode shapes. Mode shapes are the natural deformation that a part or structure would experience when it is vibrated at its natural frequency. When a loading frequency from the launch vehicle matches any of the natural frequencies of the components, resonance will occur. Resonance vibrations must be eliminated or diminished as much as possible because they are the most efficiently produced and can cause the most damage. Modal analysis is also a great way to check if the mesh and boundary conditions are set up properly. If there are frequencies that are equal to zero, the mode will need to be checked and will find that the boundary conditions are not defined properly.

To identify the frequencies that must be avoided, it is important to check the user's guide of the launch vehicle to find the frequencies it will produce. The model needs to undergo a series of modal frequencies, starting at the low end to ensure simplicity, and define all with the highest response. A goal is to reduce the modal model which can be challenging because eliminating a frequency can cause adverse effects. One of the applicable methods of sorting natural frequencies is the effective mass concept, which can be useful in ranking the relative importance nodes and determining the number of modes to be included in the modal analysis [19].

3.3.2.3 Sinusoidal vs. Random Vibrations

Not common in nature, sinusoidal vibrations are a specific vibration that involves only one tone at a specific frequency. Sinusoidal vibrations allow for very specific testing of a structure which is needed to find the natural frequencies of the material and identify specific frequency weak points. On the top of figure 3.6, a sinusoidal vibration can be seen which resembles a sine wave. Random vibrations are exactly how it sounds, there is no pattern and contain a bunch of random frequencies all at the same time. Random vibrations are probably the most common vibration and are seen in wind, automotive engines, and the white noise of TV static. When testing with random vibrations, a parameter is set to include a band of frequencies over time, similar to the bottom of figure 3.6 which shows an example of random vibration.

Random vibration has an additional difference from sinusoidal vibration. Sinusoidal vibration, because it only involves specific sinusoidal frequencies, only deals with steady-state response. Random vibration not only includes steady-state response, but also the transient effects that are seen in the beginning of a system response. These transient effects generally occur when the system suddenly is excited by an external force, and before the system reaches its steady-state frequency. The output solution of random vibration, because the system includes transient effects, is a statistical solution with sigma factors which define the probability that a certain

amount of deformation will occur in a certain direction. More on this statistical solution will be defined in section 6.4.

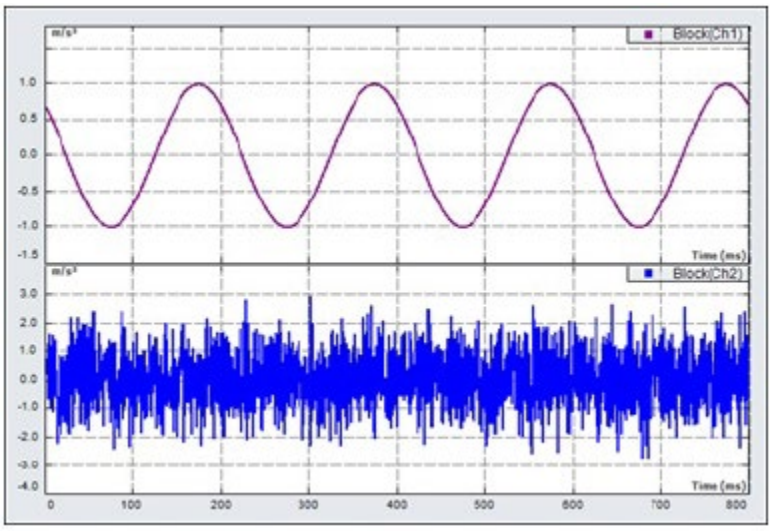

Figure 3.6 Sinusoidal vibration (top) and random vibration (bottom) [20]

3.3.2.4 Harmonic Response Analysis

Harmonic response analysis is important because it gives the ability to predict the sustained behavior of any structure which enables the ability to verify whether the system can or cannot successfully overcome resonance, fatigue, and other harmful effects of forced vibrations [19]. This analysis will only consider steady state forced vibrations, not transient. Steady state vibrations are sinusoidal vibrations that vary with time. The goal of harmonic response analysis is to generate a plot of how the component responds to a range of frequencies, common plots are displacement vs frequency. Any frequencies that peak in the plot which match the natural frequencies seen from the modal analysis are identified to check for the amount of fatigue damage it could cause. These peak frequencies are the resonance frequencies that are needed to avoid or diminish through design or material choices. Results of harmonic analysis will give a value for the maximum stress which can be combined for the static loads to predict if the stress will overcome the yield stress of the material. Additionally, the harmonic analysis results can output a value of maximum deformation which can be compared to the undeformed width to get a percentage of deformation. This percentage must be under the maximum percentage range defined in section 2.1.2.2. Moreover, the harmonic response analysis maximum deformation percentage will be outlined in section 6.3.

3.3.2.5 Fatigue Analysis

Fatigue is a challenging concept because a part might be able to withstand the stresses from the initial modal and harmonic vibrations, but after repeated loading may cause internal stresses to build and overcome the yield strength. Fatigue analysis will not predict when a crack will start, or how fast it will grow, but it will predict how many cycles a particular stress cycle is needed to induce failure [19]. Stress concentration is what causes most fatigue cracking and is expedited when the stress is high. It is common for most metals to be able survive about 1,000 loads of around 80% of their maximum levels when they do not have any areas of stress concentration. Fatigue analysis will not be completed for this project, but additional information can be found in reference [19].

3.3.2.6 Spectrum Analysis

Spectrum analysis uses the results from the modal analysis to calculate the forces in the part at a known spectrum. These forces are generally displacement and stress which are applied at random or at a specific time interval. Spectrum analysis is where the system will be tested using random frequencies for random time intervals at slowly increasing magnitudes. The three types of spectra for spectrum analysis are [19]:

- Response Spectrum
- Dynamic Design Analysis Method (DDAM)
- Power Spectral Density (PSD)

3.3.2.7 Vibroacoustic Affects

Acoustic noise can be very dangerous to humans and structures, which is a big issue with launch vehicles at launch pads. This is caused by the pressure waves from the engines being fired at launch bouncing off the ground and structures around the rocket. The noise at launch, during the two-minute liftoff and transonic climb through the atmosphere from the exhaust causes a hostile noise and vibration environment for spacecraft onboard and all of its sensitive equipment [21]. Since launch pads can see as high as 180 dB during launch, they will flood spray water across the launch pad to try and mitigate as much sound as possible to prevent damage. Vibroacoustic effects on structures include the following [21]:

- Mechanical Fatigue
- Mean Stress
- Acoustic Fatigue
- Shock and Transients
- Pyrotechnic Shock

All of the topics discussed in chapter 3 will be the main focus when conducting finite element analysis for the expulsion device. Static structural, and all of the vibrational analyses will be

conducted to find any points of failure that need to be addressed. The following chapter will talk about the modal setup, and the various checks that need to be done to ensure the model is set up correctly. There will also be a discussion about how many modes will be included and go into depth about the frequency requirements the system must be able to withstand.

4. Modal Analysis of Tank Assembly

In this chapter, the details will be outlined for the setup modal analysis which will be conducted on the propellant tank. This involves importing the geometry, meshing, setting the boundary conditions/constraints, solver output solution. When the solver is completed, a specified solution of total deformation will be generated for a number of modes. These modes will identify the natural frequencies that the geometry will be excited by. They will need to be compared to the expected launch vehicle frequencies to check whether to expect any resonance issues during loading, launch, or deployment. In addition, the mode frequencies will be used to conduct mesh convergence analysis. This involves increasing the amount of number of mesh elements and monitoring the frequency output of the modes to verify that the solver has converged on a frequency for each mode. Once the mode frequencies have converged, the participation factor and effective mass will be used to identify if the majority of the modes have been accounted for. Lastly, the mode shapes will be shown, and the strain energy density will be calculated to identify any areas of the geometry of which will see the highest displacement. If any of these areas of displacement are too large for the materials or components, an update for the geometry will be considered to decrease the displacements.

4.1 Simulation Setup

To properly set up the criteria needed to conduct any FEM analysis, the geometry must be discretized into mesh elements that represent the entire geometry as close as possible. For the modal and following analyses, the 2U sized propellant tank will be used. Solidworks was used to create the CAD geometry of the propellant tank, and Ansys Mechanical to conduct the various FEM analyses. These analyses will focus on the propellant tank with its mounting hardware support to measure how they respond to internal and external forces. All of the components attached to the tank that are needed for CubeSat flight, i.e. solenoids, power and GNC, will be ignored. This assumption will likely miss some lower frequency responses but can be negated because the scope of this project is on the integrity of the propellant tank.

4.1.1 Geometry

To start the analysis process, a CAD model of the most recent tank design must be imported into Ansys Workbench. Referencing the geometry seen in section 2.2.2, the propellant tank has been updated with the addition of a pressure sensor, safety relief valve, and flow control valves, integrated into the top and bottom plates. This update can be seen in figure 4.1.

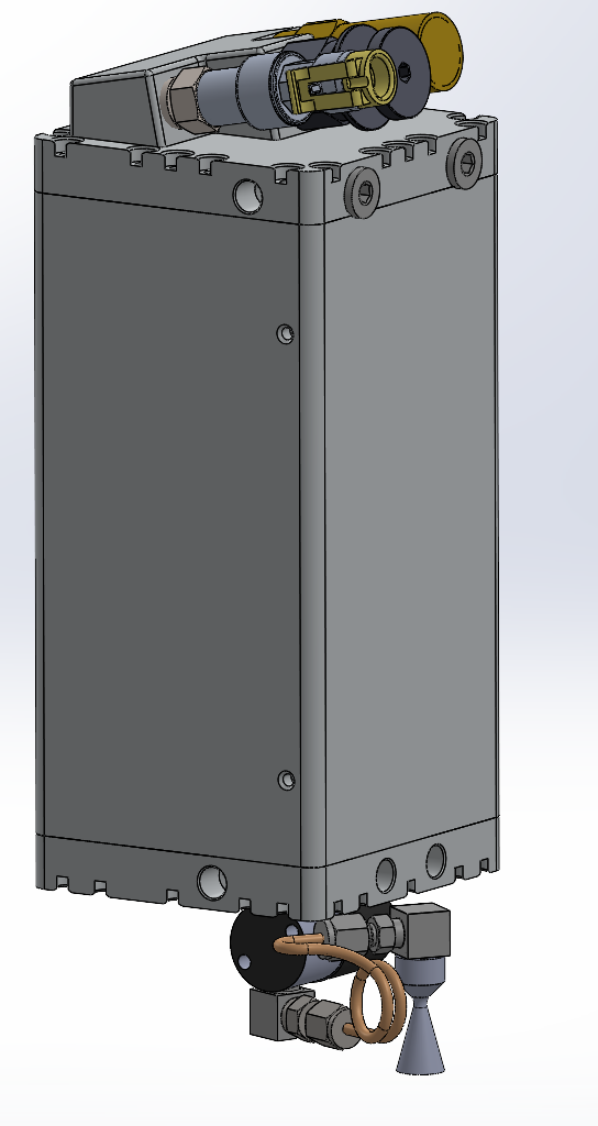

Figure 4.1 Propellant tank with sensors, valves, and thruster

4.1.2 Boundary Conditions

Using correct boundary conditions is crucial for the analysis to produce the correct results for the geometry. The system must be constrained to the exact conditions that the model will undergo during flight. For this simulation, the propellant tank will be fixed using eight cylindrical mounting points, bolts, around the body of the tank which would connect into countersunk holes in the CubeSat. These mounting points can be seen in figure 4.2. Additionally, the propellant tank will be modeled to simulate the properties of 6061 aluminum alloy.

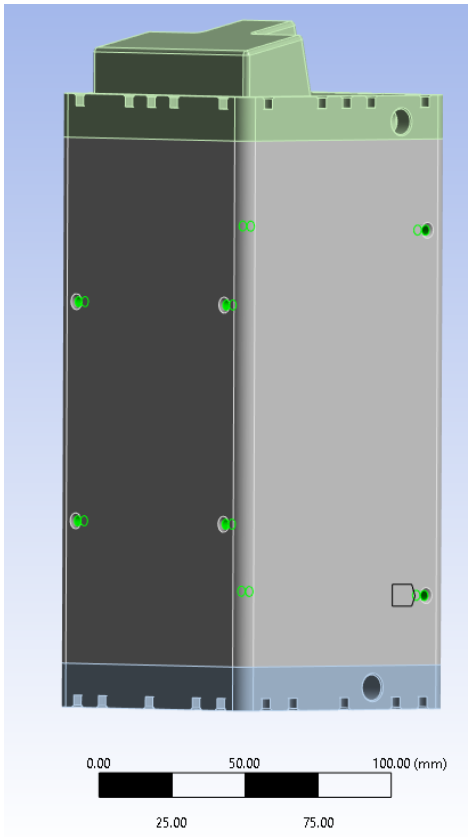

Figure 4.2 Tank bolt mounting points (in green)

4.1.3 Meshing

Meshing can be one of the hardest parts of an entire simulation and, with boundary conditions, is also the most critical. If the mesh is applied incorrectly or the cell size is too large, then the simulation can give incorrect results by large over-simplifications of the geometry. This, however, does not mean to make the cell size as small as possible. The smaller cell size increases the number of elements, and with more elements, increases the computational consumption required to solve. However, there is a point where the accuracy does not increase with the increased cell size. This point can be found by changing the cell size and checking the change in natural frequencies from the previous analysis. Computers, although they are very fast at solving equations, are limited by the hardware available to use. Simulation speed is driven by the number of CPU's, number of physical cores on each CPU, and the amount of available RAM. A higher element count will require a higher amount of RAM and will create a larger file to save. The computer used for these simulations is an Intel i9-12900K 16 core with 96 GB of RAM. It was found that using an indicated 15 cores, and selecting the distributed cores box, increased the rate of solving significantly compared to the distributed cores deselected. For example, one case took 7 minutes and 14 seconds to complete with distributed cores off, and with it on the same case solved in only 1 minute and 18 seconds.

This FEM simulation was set up in Ansys Workbench using a mechanical model block to adjust and store the geometry and mesh data. These blocks can then be referenced individually by whichever analysis to get the mesh data from. This is done to prevent repetitive recalculating of the mesh by meshing the geometry one time in the model block and then referencing the mesh in the solver blocks. An example of the setup of the modal solver blocks referencing the mesh block can be seen in figure 4.3.

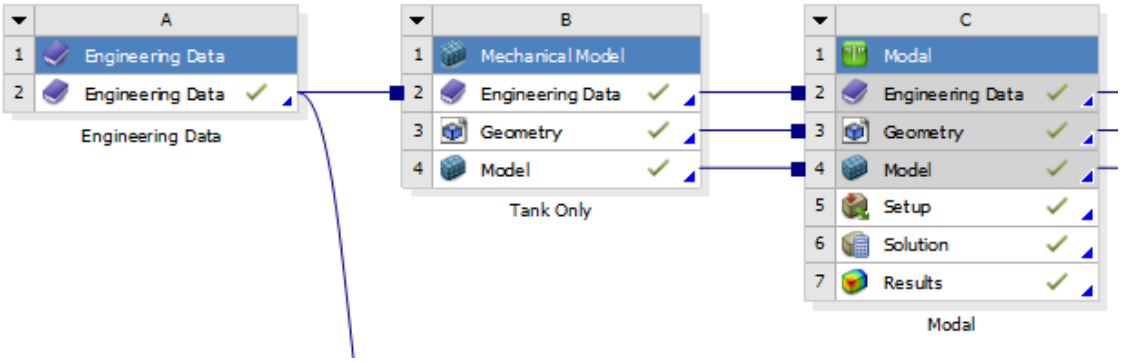

Figure 4.3 Ansys Workbench with the modal analysis referencing the geometry mesh block

The initial mesh was created by adding constraints to enable manual refinement of specific mesh types per body or surface. In this simulation, body size control was used to set the propellant tank assembly to a target cell size of 8 mm. This will be the starting mesh so that a baseline modal analysis can be completed. This baseline analysis will be used for a few verifications. The first verification is to check if the boundary conditions were set up properly. If one of the modes from the modal analysis calculates to have a zero frequency, then this is a clear indication that the geometry is not mounted or fixed properly. The second verification will be used to check whether the element sizes are within a reasonable size to capture a closely accurate frequency range. This is done by not only changing the cell sizes, but also the types of elements being used. For this simulation, the element orders of linear or quadratic will be analyzed with the element method of tetrahedron. The hexahedral element method will not work for this geometry as the mesh generation quality is too poor. This decision was made by Ansys as it calculated a large number of deformities in the hexahedral elements which did not properly define the complex geometry. In addition to order, the cell sizes will be decreased until the mode frequency change from the increased element count of the previous analysis is less than a 2-3% difference. This method of verification is called mesh convergence analysis. The initial mesh of the propellant tank at a 4 mm cell size can be seen in figure 4.4.

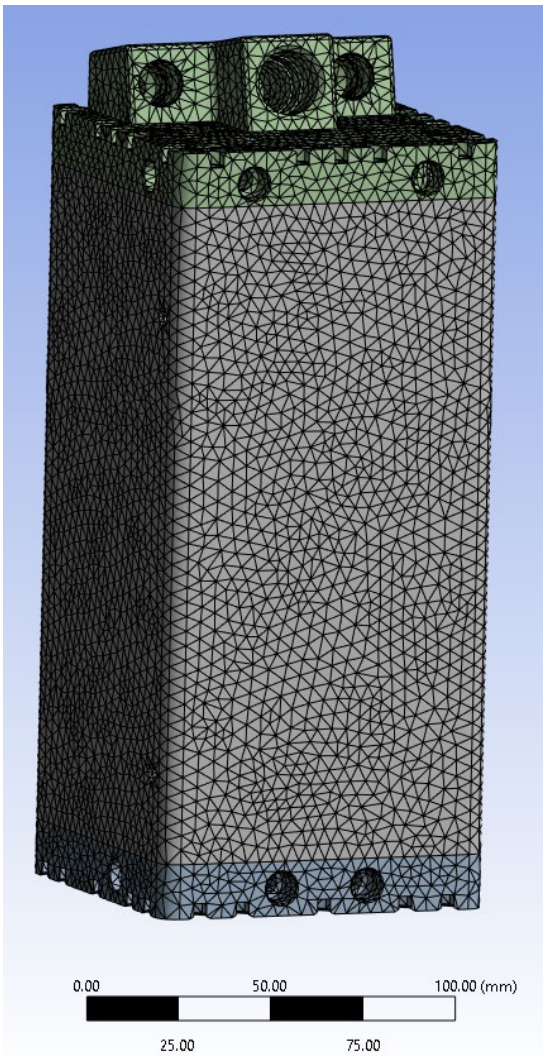

Figure 4.4 Propellant tank quadratic mesh at 4 mm

4.2 Results of Modal Analysis

Modal analysis was performed initially on the propellant tank and since the mesh was already completed in the mechanical model block, the mesh was already ready to use when the modal block was added. When setting up the modal analysis, the boundary condition must be defined. This is where the 8 mounting points were selected to be cylindrical supports as seen in figure 4.2. A few cases were run during the mesh convergence process to find an element size and method that gave an accurate result which did not take an excessive time for the computer to solve. Once a mesh size and method have been converged on, the maximum number of modes can then be verified to be sufficient enough by the use of the participation factor and effective mass. Additionally, these frequencies will be compared to the launch vehicle requirements to verify the modes include all of the possible frequencies that the structure can experience during launch.

4.2.1 Mesh Verification

The initial modal analysis settings had the maximum modes to find set to 15. This was done because the resulting mode frequencies will be recorded and checked against the results of the previous mode with different target element size and element methods. Table 1 shows the changes between the modes as the target element size is made smaller, as well as changing between linear and quadratic. An element size of 8mm with a linear order and tetrahedron method was used first to set a baseline. It was apparent almost immediately that the linear method, although it solved faster, seemed to be less accurate when compared to the same size but with the quadratic order. In addition to the lack of accuracy, Ansys Mechanical also gave warning messages about using a linear order with the current settings and parameters. For the sake of comparison, both the linear and quadratic orders were run with decreasing target element size until the frequencies began to converge. Table 1 shows the results from the quadratic order, and table 2 shows the results from the linear order. Almost immediately, the modes for the quadratic began to start to converge to a value as the element count increased, which can be seen in figure 4.5. Each of the quadratic cases has a percentage difference of less than 1%, where linear stays at about 2%. In fact, looking at figure 4.6, the linear cases are slower to converge towards a value. Looking at table 1, since the change is within the 2-3% difference it needed to be, the decision was made to use case 2 with the 6 mm size and quadratic order. The difference of mesh sizing from 6 to 2 mm can be seen in figures 4.7 & 4.8.

Table 2 Mesh convergence quadratic order element parameters

Mesh Convergence Analysis - Quadratic Element Order											
Case	Target Element Size [mm]	Percent Difference (Mode 15)	Time to Solve	Element Count	Node Count	Mode 1 [Hz]	Mode 2 [Hz]	Mode 3 [Hz]	Mode 8 [Hz]	Mode 12 [Hz]	Mode 15 [Hz]
Baseline	8	---	9 sec	40177	71944	4135.6	4324	4676.9	7686.6	9083	10806
2	6	0.56%	12 sec	61528	106265	4102.6	4297.5	4648.1	7649.4	9036	10746
3	5	0.16%	15 sec	82820	139442	4096.9	4284.2	4639.4	7638.7	9015.6	10729
4	4	0.35%	26 sec	139349	225532	4074.9	4266.2	4620.8	7607.7	8991.1	10691
5	3	0.21%	4 min 30 sec	301198	465589	4061.6	4255.3	4609.1	7594.9	8969.7	10669
6	2	0.20%	10 min 56 sec	953467	1405424	4047.2	4239.4	4596.3	7578.5	8943.8	10648

Table 3 Mesh convergence linear order element parameters

Mesh Convergence Analysis - Linear Element Order											
Case	Target Element Size [mm]	Percent Difference (Mode 15)	Time to Solve	Element Count	Node Count	Mode 1 [Hz]	Mode 2 [Hz]	Mode 3 [Hz]	Mode 8 [Hz]	Mode 12 [Hz]	Mode 15 [Hz]
Baseline	8	---	6 sec	40177	11297	4694	4919	5902.6	8674.6	10174	12003
2	6	2.43%	6 sec	61528	16280	4528.6	4768.8	5440.1	8363.4	9824.4	11711
3	5	1.02%	6 sec	82820	21013	4471.5	4693	5320.8	8260.8	9691.5	11592
4	4	1.88%	7 sec	139349	33107	4371.7	4588	5089.3	8063.9	9520.3	11374
5	3	1.88%	11 sec	301198	66172	4288.8	4500.4	4915.9	7922.8	9370.9	11160
6	2	1.97%	31 sec	953467	192619	4182.6	4390.6	4760.6	7760.1	9182	10940

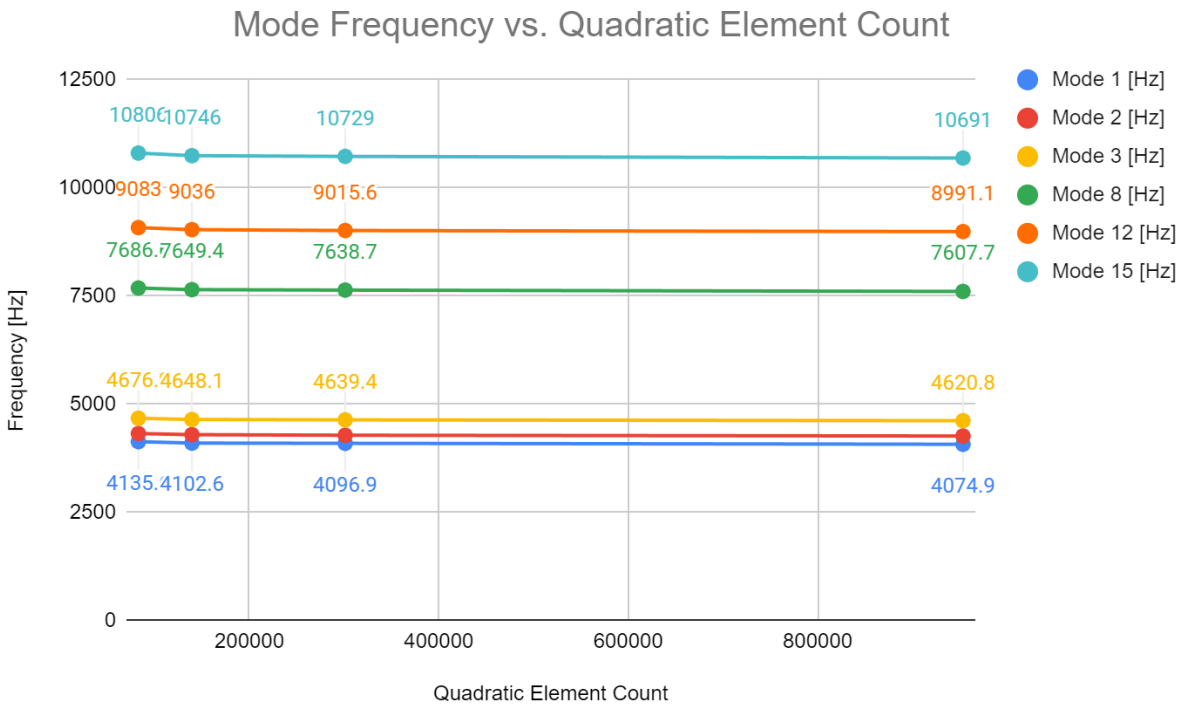

Figure 4.5 Frequency vs. quadratic element count for 6 modes

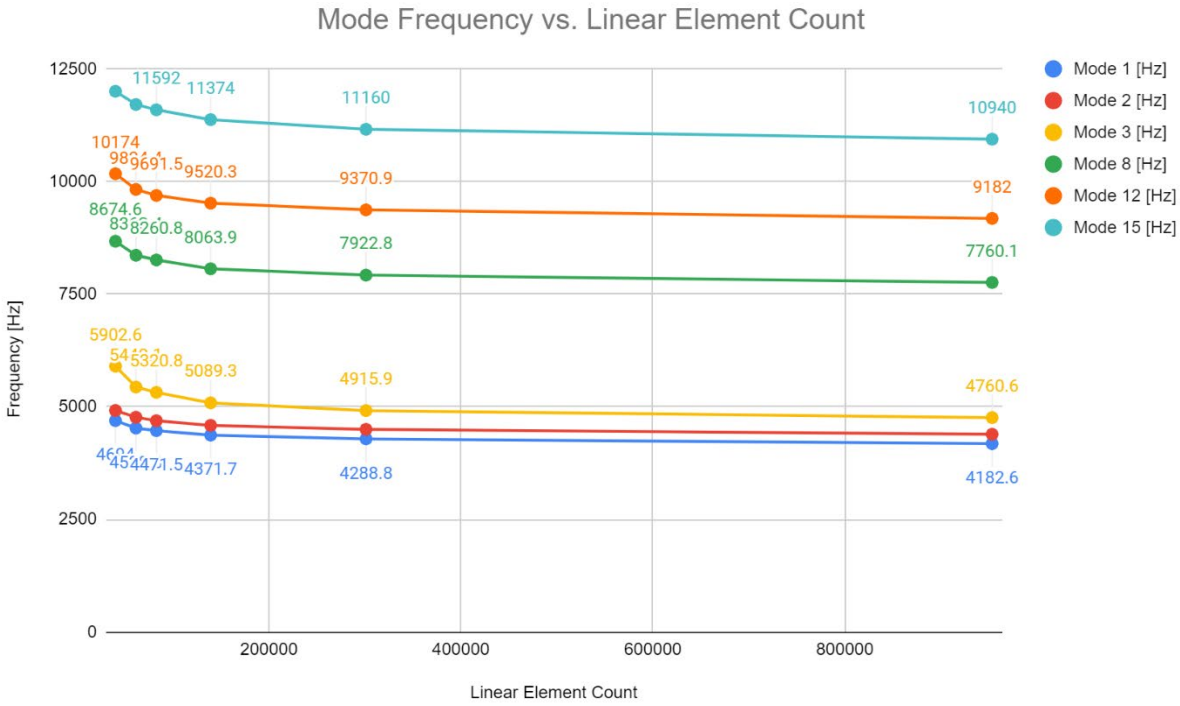

Figure 4.6 Frequency vs. linear element count for 6 modes

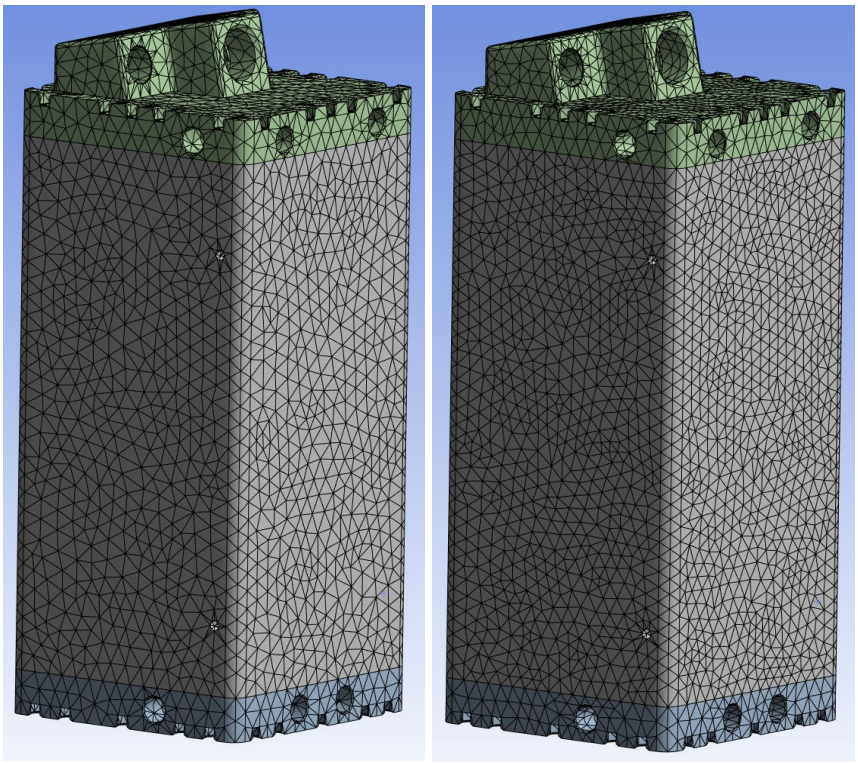

Figure 4.7 Quadratic tetrahedron mesh of 6 mm (left) & 5 mm (right)

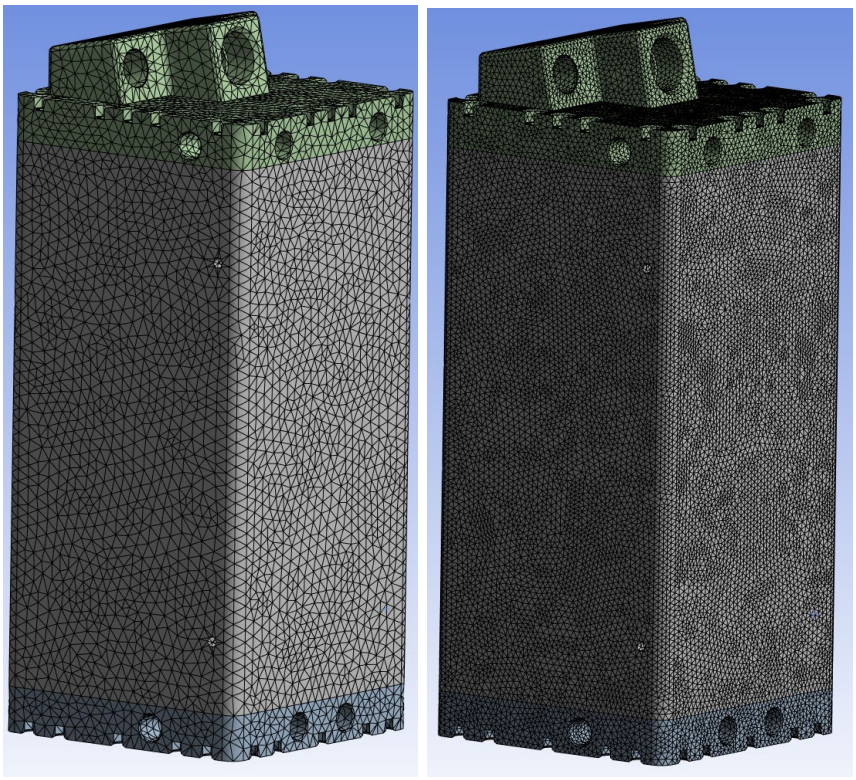

Figure 4.8 Quadratic tetrahedral mesh of 4 mm (left) & 2 mm (right)

4.2.2 Participation Factor and Effective Mass

Other important factors to check with modal analysis are the participation factor and effective mass. These values can be found as a solution output which is selected to be the participation factor summary. The participation factor is used to find any modes which will cause excitement in a certain direction from an external force. This is important to know because if the launch vehicle is known to produce a certain force in the direction, then the tank will experience resonance which could damage components. This simulation did not see any high translational movement about any x, y, or z axis, however, there were many modes which had reasonable rotational motion in 1 or 2 axes at a time, but their motion will not cause any damage.

Effective mass is useful because it can help determine if the solution contains enough modes. This is done by calculating the effective mass that is experiencing displacement per mode. All of the mode displacements are summed per direction and should theoretically equal the total mass. This, however, is never true because the points at which are fixed or constrained will not contribute mass to the effective mass. From the simulation with 15 modes, the effective mass percentage was between 92 and 97% of the total mass.

4.2.3 Strain Energy Density

Strain energy density is important when wanting to find possible failure points so that they can be fixed inside the CAD model. Strain energy density is the strain energy, also known as the potential energy, divided by the volume of the geometry. This works because it calculates the highest areas of strain per mode and highlights it within the model. With any of the highlighted areas that are where high-risk components are located, the directional of the strain can be used to identify how the model can be fixed. For this simulation, all of the high strain energy density areas were within the mounting points and will be monitored closely during static structural analysis for any failure points. Figure 4.9 shows the elements in orange/red which experience a high mJ of strain energy.

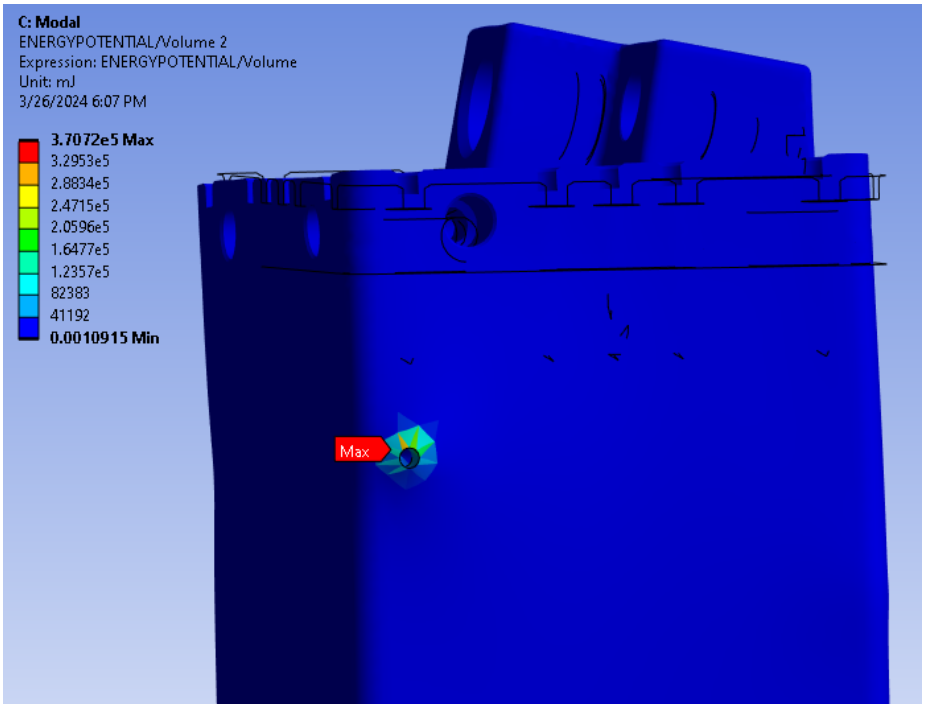

Figure 4.9 Close up of strain energy density

4.2.4 Mode Shapes

Mode shapes are the shapes of deflection that a material will generate when it is matched with one of its natural frequencies. These mode shapes take on the properties of a sine wave, and with higher frequency more waves are produced in the material. This becomes more apparent when comparing a low and high frequency mode. Table 3 shows the results from the modal analysis of the propellant tank. Mode 1 looks like it is starting to have deflection but not quite a sinusoidal shape, mode 7 looks like a half sine wave period, and mode 15 looks like a full sine wave which can be seen in figure 4.10.

Table 4 Natural frequency mode shapes

Mode Shape	Frequency (Hz)
1	4061.9
2	4254.9
3	4609.2
7	6601.8
12	8969.5
15	10670

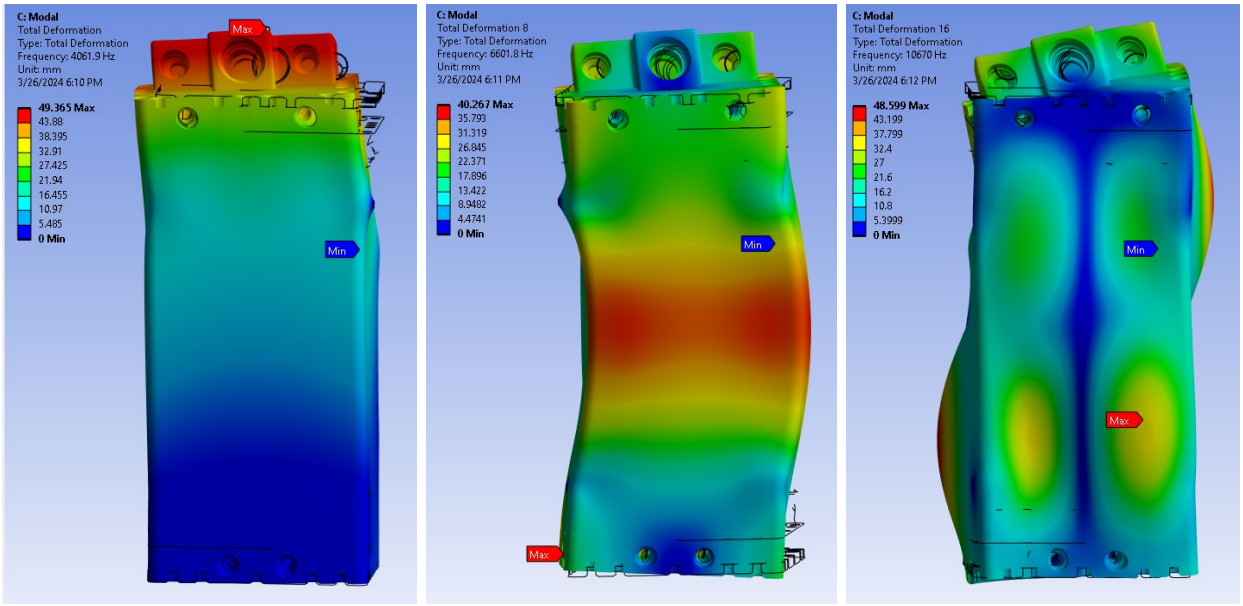

Figure 4.10 Mode 1: 4061.9 Hz (left), mode 7: 6601.8 Hz (center), mode 15: 10670 Hz (right)

4.3 Modal Analysis Results Discussion

With the modal analysis results showing the natural frequencies of the system, these frequencies will need to be compared to the Falcon 9 rideshare launch requirements to ensure system compliance. According to the rideshare user guide requirements, the system payload must have no elastic natural frequencies below 40 Hz [24]. From the modal analysis it was found the first mode, or lowest natural frequency occurs at a frequency of 4061.9 Hz, well above the minimum requirement of 40 Hz. These results ensure that the system is safe to continue further analysis of static structural quasi-static loading.

5. Static Structural Analysis of Tank Assembly

In this chapter, the propellant tank will undergo static structural analysis to identify the amount of displacement and equivalent stress and strain when the tank is under operational pressure. For displacement, the solution can be used to identify the amount the tank will swell from the high expected pressures and where it will occur. More importantly, the result from the stress solution will be used to identify where and what pressure the material of the tank is predicted to yield. Each material will have a set yield strength value which will be divided by the value of stress calculated from the simulation at a defined pressure. This ratio is the safety factor. For this simulation, the yield strength of the material will be referenced instead of the ultimate tensile strength because at the yield strength, permanent deformation occurs and will inherently cause permanent damage to the tank. Ansys has a solution output which automatically calculates the safety factor based on the amount of stress from the defined pressure and the ratio of that equivalent stress to the yield strength of 6061 aluminum. As previously stated in section 2.1.1, the safety factor margin should be between 1.5 and 1.8. Any results that do not fall within this ratio will require the geometry to be reworked.

5.1 Static Structural Setup

The setup of static analysis is exactly the same as what was done with the modal analysis. Since the geometry and mesh block was already created from the modal step, the same data can be forwarded to the static block. Since the body of the CubeSat is not being referenced in this simulation, the boundary conditions will need to match the same conditions as if it was still integrated into the chassis. This is done by defining the bolted connections between the tank and chassis to be cylindrical supports to prevent movement in radial, axial or tangential directions.

Since this is a pressurized propellant tank that will integrate inside a CubeSat on a lunch vehicle, the analysis will need to define the internal pressure and the external launch loads at which the tank will experience. To do this, each of the faces that are in contact with the expected pressure are selected and defined to the chosen pressure of 750 psi. Additionally, from the launch vehicle requirements, it is known that the CubeSat will experience a quasi-static load factor of 10 g in the axial direction and 17 g in the lateral [24]. To define which directions will be axial or lateral, the coordinate system definition for the launch vehicle must be compared to the coordinate system definition in Ansys. The coordinate system defined from SpaceX Falcon 9 can be seen in figure 5.1, where the PLx direction is axial, and the PLy and PLz are lateral. This correlates to the coordinates in Ansys by:

- Launch Vehicle: PLx | Ansys: -y
- Launch Vehicle: PLy | Ansys: -z
- Launch Vehicle: PLz | Ansys: +x

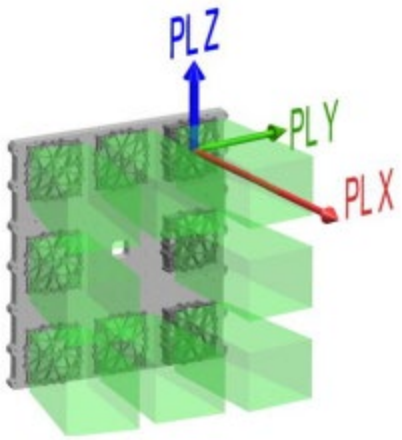

Figure 5.1 SpaceX Falcon 9 CubeSat dispenser orientation [24]

The faces defined for the pressure load can be seen in figure 5.2, and the equivalent load from the launch vehicle in figure 5.3. The solution outputs are set as follows:

- Total Deformation
- Equivalent Elastic Stress
- Equivalent Stress
- Stress Tool for Maximum Principal Stress (For Safety Factor)

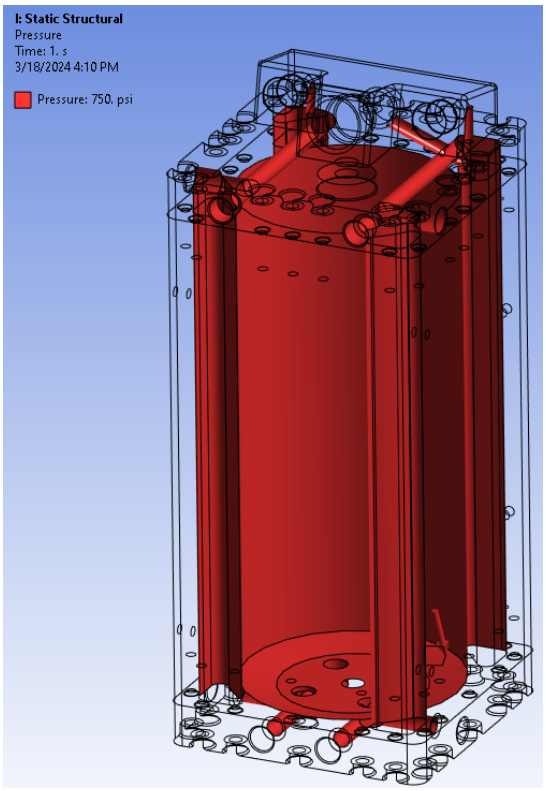

Figure 5.2 Static structural interior face selection for pressure load definition

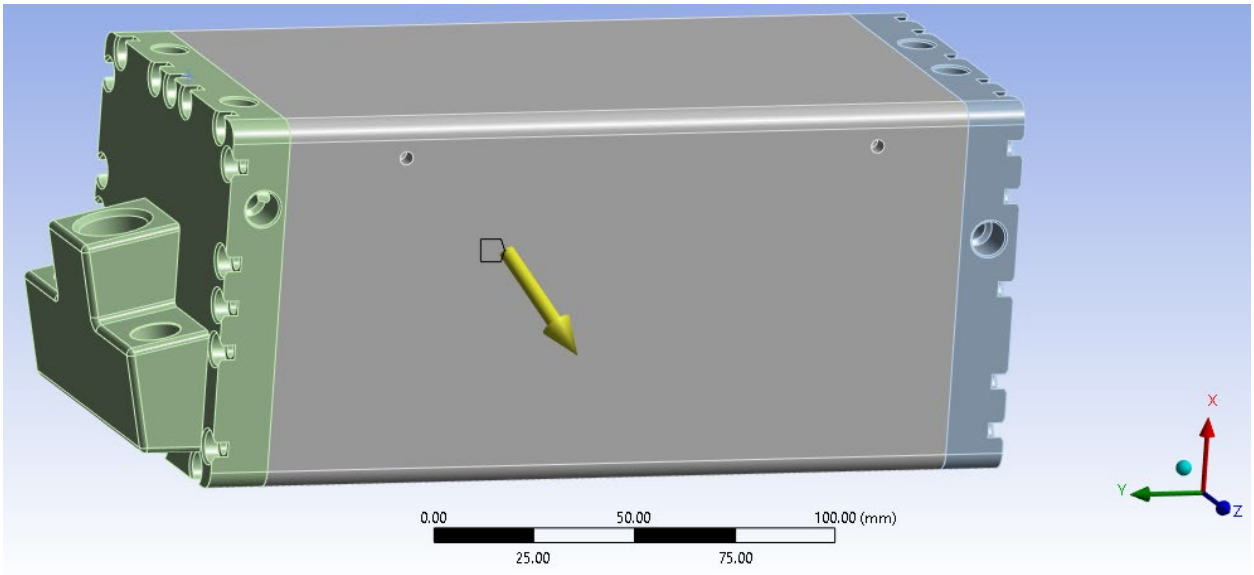

Figure 5.3 Combined quasi-static loads from the falcon 9 launch vehicle

5.2 Results of Static Structural Analysis

For the static analysis with the pressure set to 750 psi, the numerical results can be found below in table 4. Figures 5.4 to 5.7 show the solution outputs from a front whole and front section view with the tank cut in half to reveal the internal details. The aluminum material used for the Ansys simulations has a yield strength of 280 MPa, at 750 psi the maximum equivalent stress is 146.51 MPa. With the material yield strength divided by the equivalent stress, the safety factor is returned to be 1.91. Since the safety factor is above the 1.5 to 1.8 range, it is known that the tank is marginally overbuilt and has excess mass that could potentially be removed.

Table 5 Static structural results at 750 psi

(750 psi)	Maximum	Average	Minimum
Total Deformation	$3.266x10^{-2}\ mm$	$1.253x10^{-2}\ mm$	$0\ mm$
Equivalent Elastic Strain	$2.706x10^{-3}\ \frac{mm}{mm}$	$2.283x10^{-4}\ \frac{mm}{mm}$	$8.951x10^{-7}\ \frac{mm}{mm}$
Equivalent Stress	$146.51\ MPa$	$15.59\ MPa$	$3.266x10^{-2}\ MPa$
Safety Factor	-	-	1.91

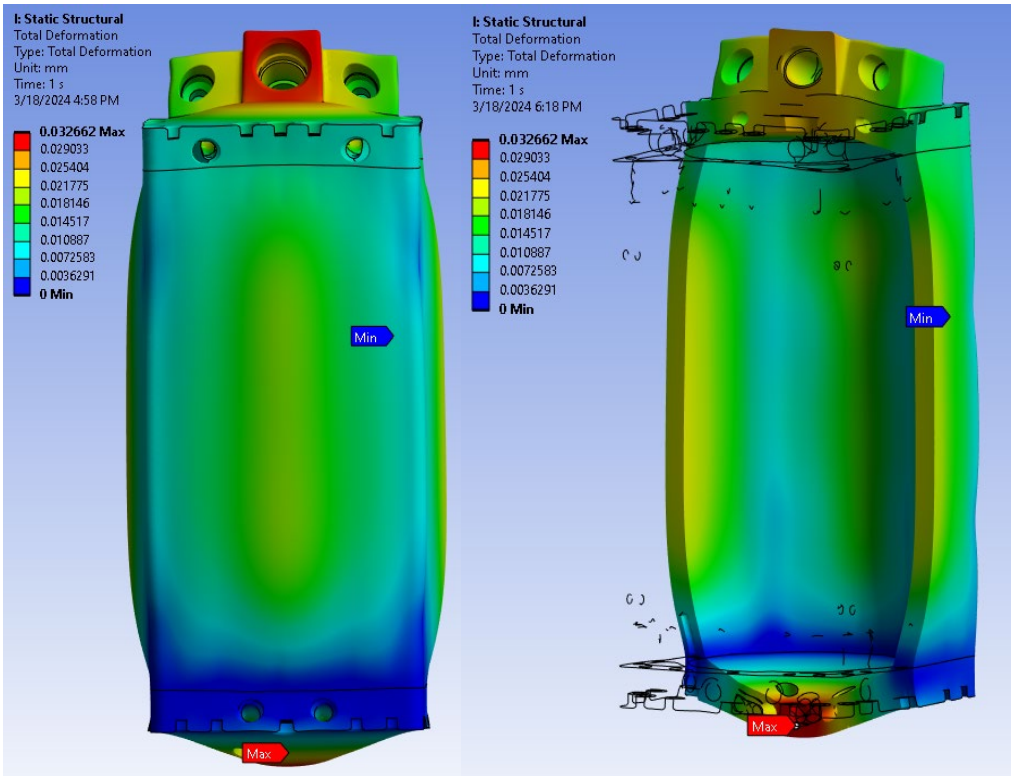

Figure 5.4 Total deformation at 750 psi (section view right)

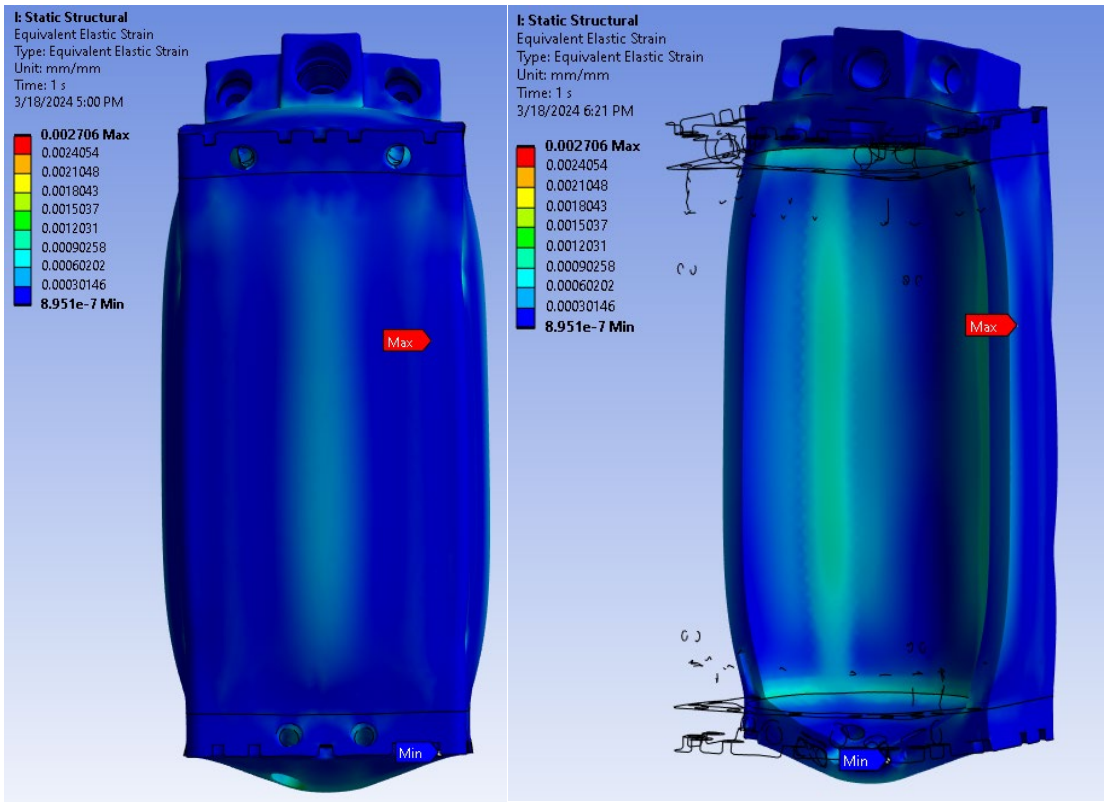

Figure 5.5 Equivalent elastic strain at 750 psi (section view right)

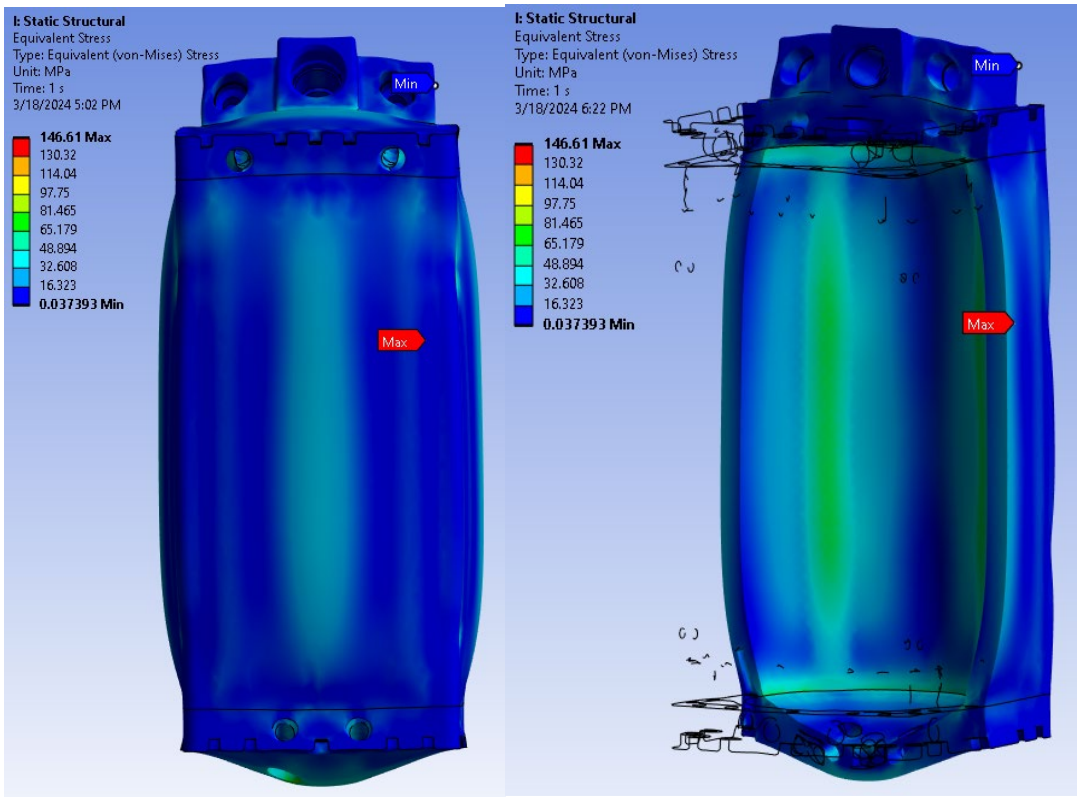

Figure 5.6 Equivalent von-mises stress at 750 psi (section view right)

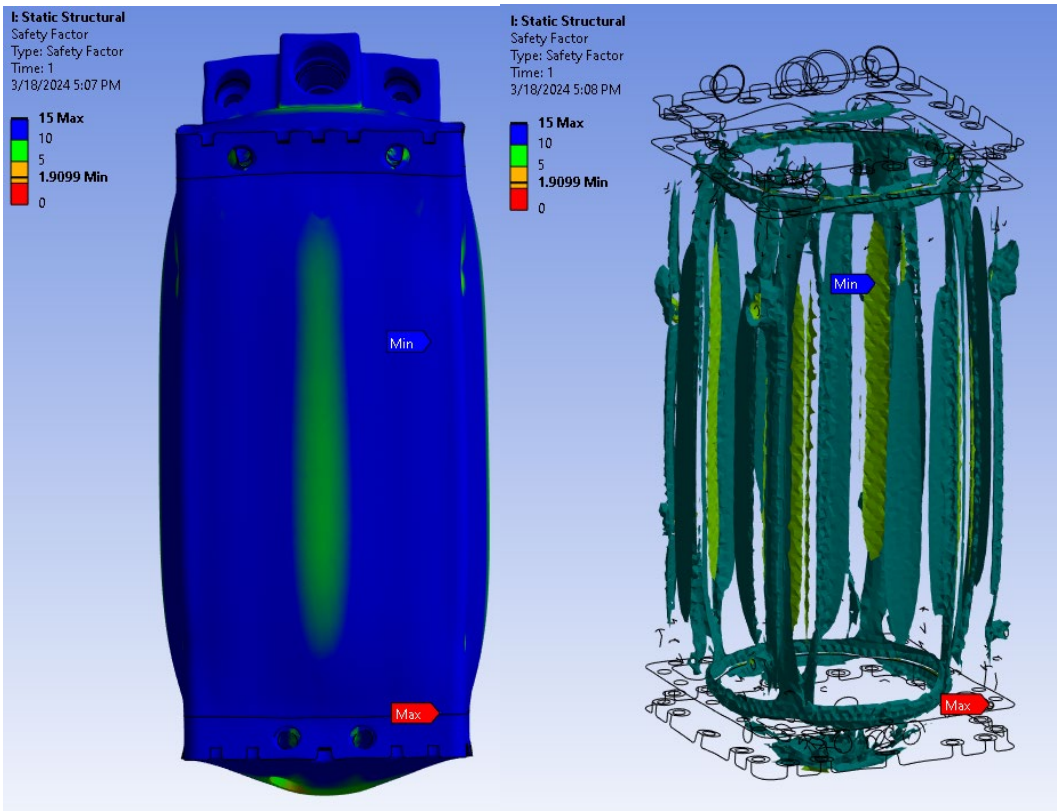

Figure 5.7 Safety Factor at 750 psi (isosurface section view right)

Additional analysis of the results from the isosurface safety factor in figure 5.6, it has identified the highest stress points at the bolted connections as well as the surfaces between the corner pocket and the inner cylinder. For the inner cylinder, the piston x-rings need to have enough spring stretch to remain sealed when the cylinder walls expand by 0.033 mm. The bolted connection points, seen in figure 5.8, are potentially concerning since the drilled holes create a few weak points near the pressurized corner pockets. In the next section, the mounting holes will be moved from the tank body to the top and bottom plates to test if removing them can increase the safety factor.

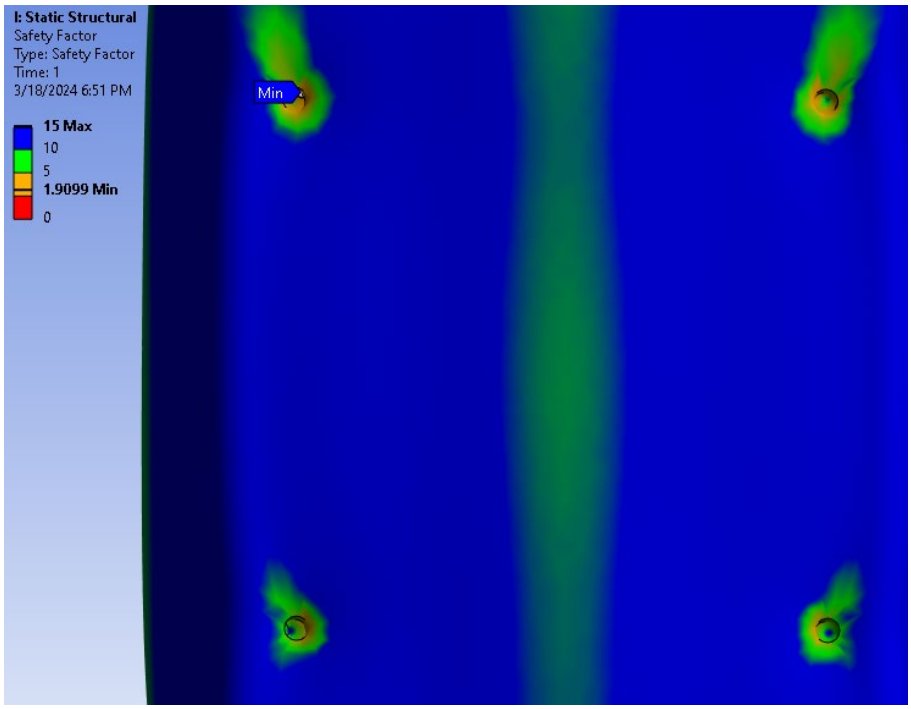

Figure 5.8 Close up of potential issues with connection points

5.3 Static Structural Verification

To verify whether or not the connection points are causing a decrease in safety factor, the bolt points will be moved from the body of the tank to the top and bottom plates. This update of the design can be seen in figure 5.9 highlighted in green, and if the result finds the bolts are weakening the structure, the updated design will be used and require the modal analysis to be redone.

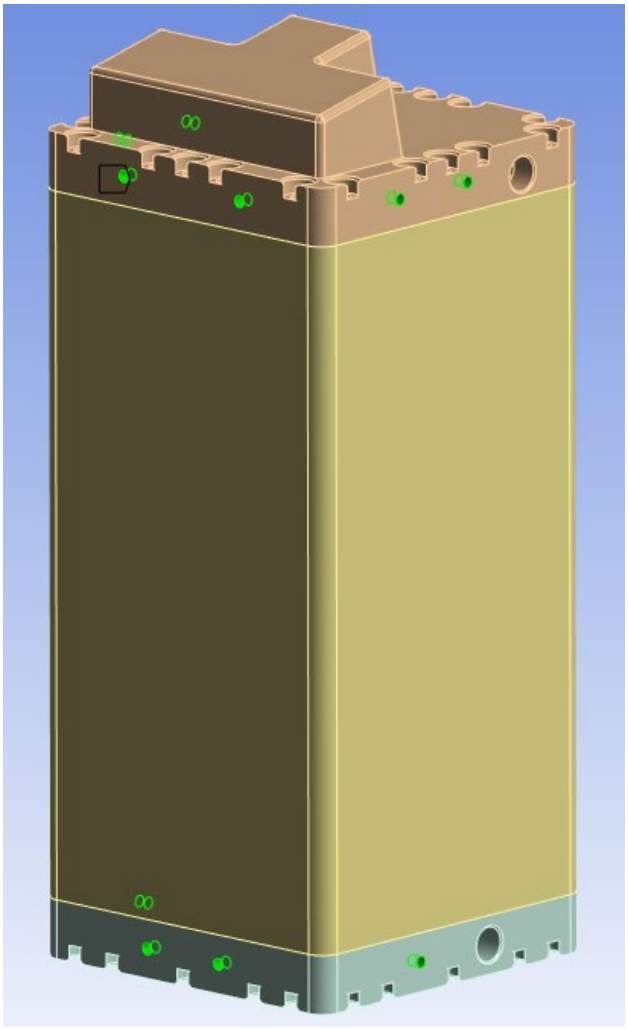

Figure 5.9 Updated tank design with mounting holes moved from body to top/bottom plates

From table 5, the results have changed by a small, negligible amount which means that the integrity of the tank did not change with the movement of the mounting holes. This allows the assumption to be made that the holes themselves are the source of the high stress and should be investigated further. Figure 5.10 shows the updated mounting holes and how the low factor of safety followed the holes and continues to be concentrated about the holes. Since the hole placement had a negligible impact on the stress levels, the analysis will continue with the holes at their original position seen in figure 4.4.

Table 6 Updated tank mounting holes at 750 psi

Total Deformation	$2.963x10^{-2}\ mm$	$1.247x10^{-2}\ mm$	$0\ mm$
Equivalent Elastic Strain	$2.562x10^{-3}\ \frac{mm}{mm}$	$2.296x10^{-4}\ \frac{mm}{mm}$	$5.547x10^{-7}\ \frac{mm}{mm}$
Equivalent Stress	$147.62\ MPa$	$15.669\ MPa$	$2.488x10^{-2}\ MPa$
Safety Factor	-	-	1.90

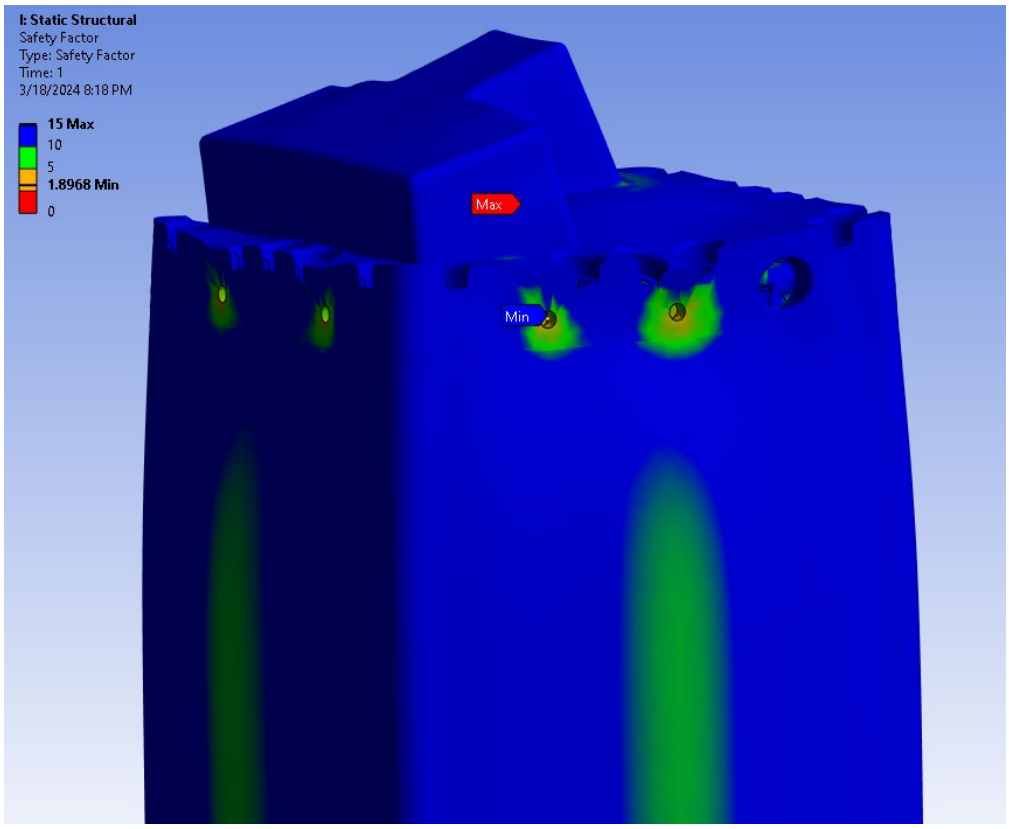

Figure 5.10 Updated mounting holes at 750 psi

5.4 Static Structural Analysis Results Discussion

After conducting the static structural analysis, it is important to compare them with the requirements from the Falcon 9 rideshare requirements, as well as all of the other requirements stated in chapter 2. As previously stated, the payload was subjected to an internal pressure load of 750 psi along with an external axial and lateral load of 10 g's and 17 g's respectfully. The safety factor at these conditions was found to be 1.9 which, comparing to section 2.12, shows that the system passes static load requirements found from the Air Force propellant tank structural requirements of a factor of safety between 1.5 and 2.2. Additionally, the system passes the structural requirements from the Falcon 9 Rideshare user guide of having a minimum of 1.1 factor of safety and meets the requirements of a type 1 pressure vessel with a 1.5 factor of safety. With the successful compliance of the static structural requirements, the system will continue to harmonic and random vibrational analysis.

6. Harmonic and Random Vibration Analysis of Tank Assembly

In this chapter, the tank will undergo both harmonic and random vibration analysis. Harmonic analysis, also known as sine sweep, is not required by the launch vehicle requirements but will still be completed to ensure rideshare compliance. Both harmonic and random vibration will use mode superposition which is highly efficient. This information is pulled from the solver output from the modal solution found in chapter 4.

6.1 Harmonic Simulation Setup

For the harmonic vibration analysis setup, the modal results will be used to set a base for the harmonic solver. This is achieved by linking the modal results block to the harmonic input environment block. The analysis settings require a minimum and maximum frequency, these are based on the lowest and highest mode frequencies found in chapter 4. The range is set between 4109 and 10670 Hz. Another important control to enable is the cluster results option. This number was set to 8 which will cluster 8 resulting points around the peaks of the frequency response plot. The frequency response plot, which compares amplitude in mm to frequency in Hz, is called a Bode plot, and shows where the largest displacements in a certain direction will peak at a certain frequency. In the results section of the Bode frequency response plot, Ansys automatically will indicate the frequency at which the highest peak occurs along with the phase angle at which it occurs. This frequency and angle can be used to create an equivalent stress response solution which will show how much the amplitude of displacements and where in the geometry it occurs.

A very important control that must be added for the analysis to work properly, is the need for damping. The damping for this simulation was set to be 2% direct input, this is an assumption, but it will ensure the results do not run away towards infinity. Using a 2% damping constant was chosen as it was recommended from the Ansys tutorials. Additional assumptions are:

- All inputs are sinusoidal
- Transient vibration effects are ignored
- Steady-state response, all harmonic loads are applied for a long time

The external loads applied are the same axial and lateral loads seen in section 5.1 and can be seen in figure 6.1. Do notice that the force is labelled Axial acceleration, but it is the total velocity vector of the axial and lateral combined.

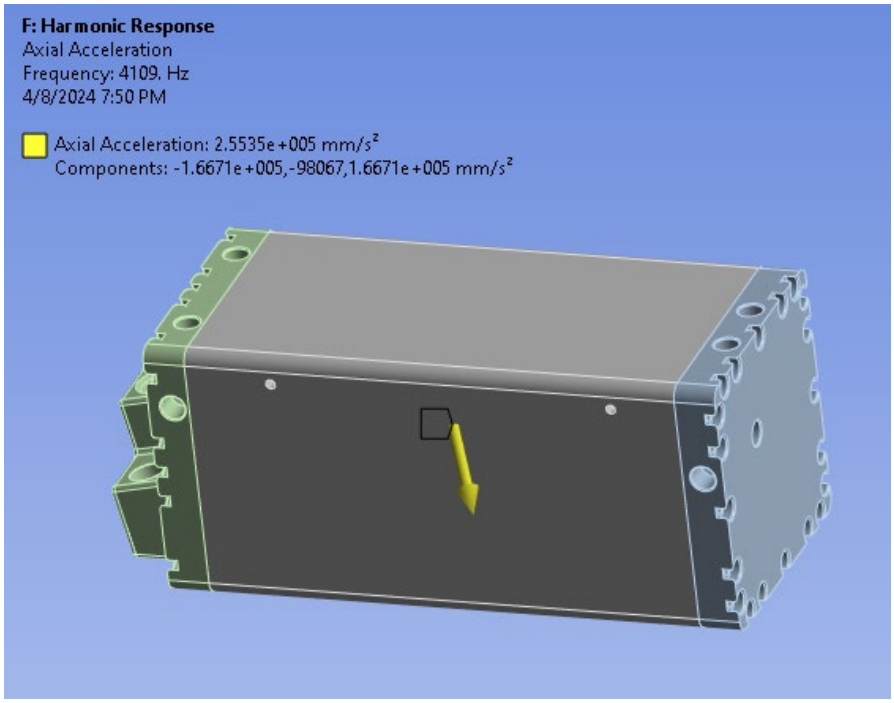

Figure 6.1 Acceleration vector load from the falcon 9 launch vehicle

6.2 Harmonic Analysis Results

The results of most interest are the amount of deformation a certain direction will experience at different frequencies. For this simulation, the directions of interest are the x axis, which is the lateral direction, and the y axis, which is the axial direction. The output solver has created a Bode plot for each of these directions as well as a directional deformation in each direction. In figure 6.2, it can be seen that the amplitude peaks twice at 4297 Hz and 5482 Hz. Ansys allows the frequency response to create a contour plot which identifies where in the geometry experiences the highest amount of deformation. In this case, figure 6.3 shows the lateral direction deformation at a frequency of 4249.7 Hz and a phase angle of 82.242°. These values are automatically selected when creating the contour plot because this is the highest peak from the

Bode plot. The tank only experiences a displacement of 0.003 mm in the lateral direction which is almost negligible.

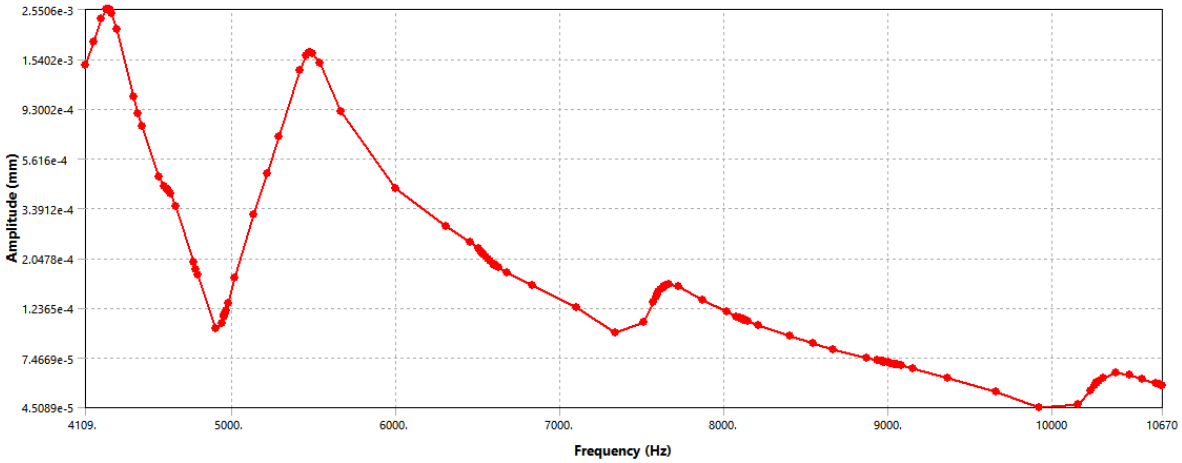

Figure 6.2 Frequency response for directional deformation x axis (Lateral)

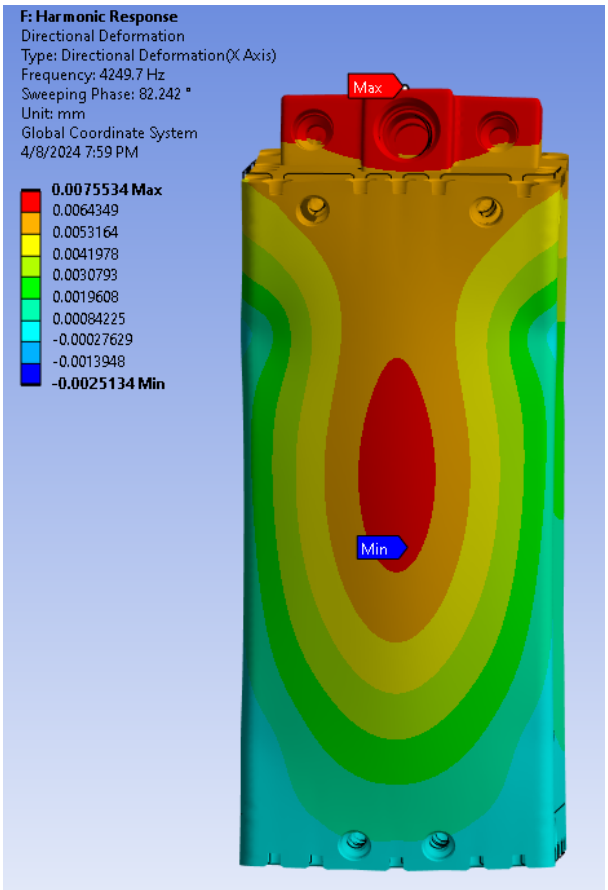

Figure 6.3 Directional deformation in the x axis

The same process was completed for the axial direction which can be seen in figure 6.4 where the Bode plot shows a single maximum frequency peak at 6523.8 Hz and phase angle of -88.392°. Figure 6.5 shows the contour plot for the axial direction at this frequency and phase angle. In the axial direction, the tank on experiences a displacement of 0.003 mm which, similar to the lateral direction, is almost negligible.

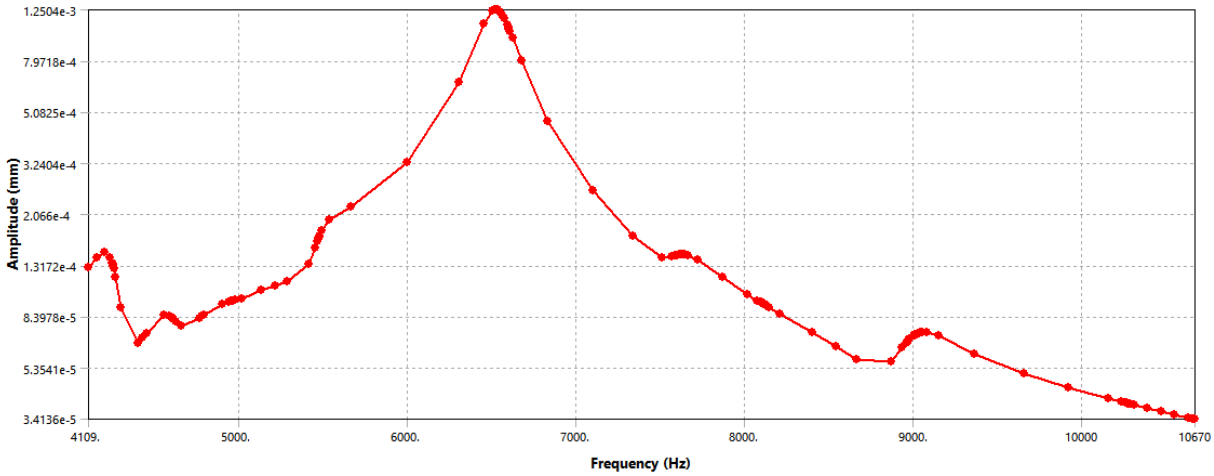

Figure 6.4 Frequency response for directional deformation y axis (axial)

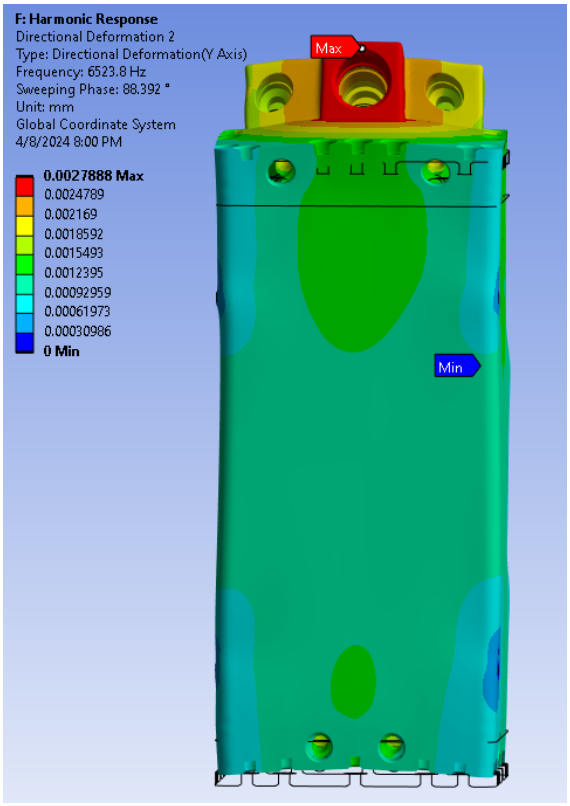

Figure 6.5 Directional deformation in the y axis

Using the same frequency and phase for each of the lateral and axial directions, the equivalent stress can be calculated and shown in a contour plot. The contour plot for the lateral direction can be seen in figure 6.6 and axial in figure 6.7. These contour plots both show that there is a high density of internal stresses around the mounting fasteners. This is to be expected since the fasteners do not move, and the rest of the material is unrestricted.

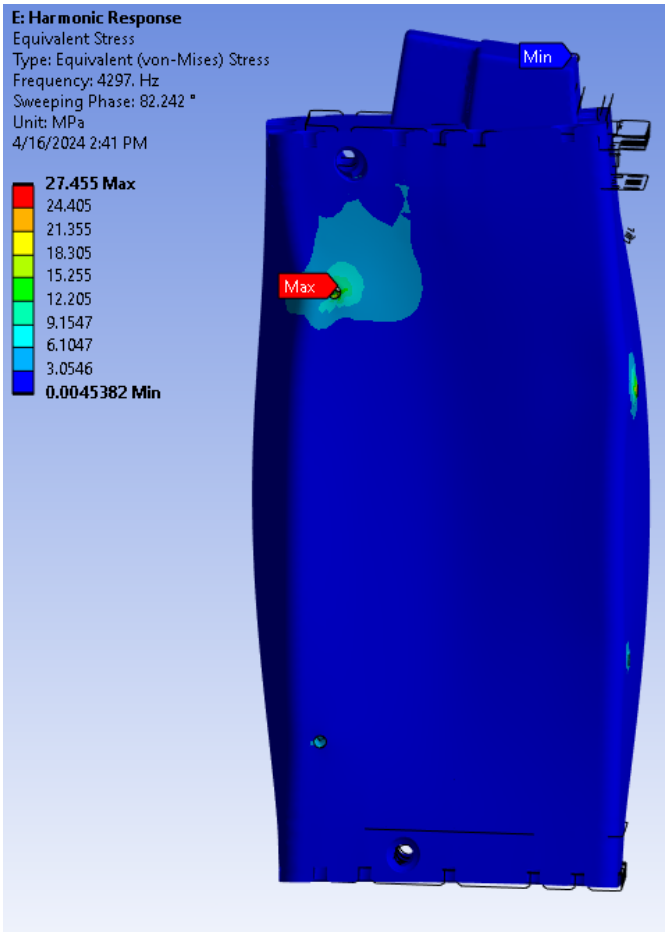

Figure 6.6 Equivalent stress at 4297 Hz and 82.242° phase angle (lateral)

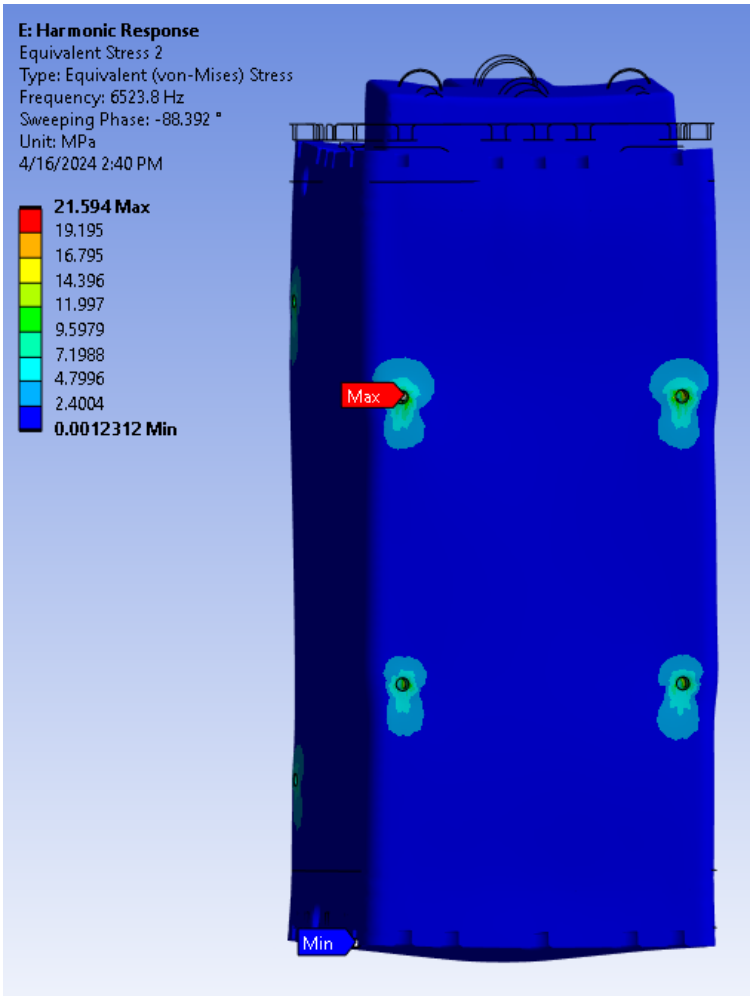

Figure 6.7 Equivalent stress at 6523.8 Hz and -88.392 phase angle (axial)

6.3 Harmonic Analysis Results Discussion

With the Falcon 9 rideshare requirements, the results from the harmonic analysis must be compared to ensure that the system is compliant. During the harmonic analysis, the system was subjected to quasi-static an axial load of 10 g's and a lateral load of 17 g's which was given by the rideshare requirements. Looking at both the x and y axis frequency response plots, it was found that the frequencies of highest deformation occurred at 4397 Hz and 6523.8 Hz. At both of these frequencies, the highest deformation recorded a distance of only 0.003 mm in either direction. To compare this to the maximum allowable deformation from section 2.1.2.2 , the percentage calculation must first be defined. The percentage is calculated based on knowing the width of the tank to be 95 mm under no loads. With the distance of deformation, in this case it is 0.003 mm, divided by the width of the tank of 95 mm and multiply by 100. The resulting percentage is 0.0032% which, compared to the range from section 2.1.2.2 of between 1.18 and 1.23%, is well below the maximum allowable deformation.

6.4 Random Vibration Setup

The random vibration analysis was set up to specifically test the maximum predicted environments at specified frequencies. These values can be seen in table 6, which were used in the Ansys analysis settings. To start, a power spectral density (PSD) G acceleration solver was set up. In the load data box, the table 6 frequencies and environments were manually entered which recreated the MPE plot seen in figure 6.8. The output of the random vibration analysis, although the contour plots look similar to the ones from the harmonic solution, have a few major differences. Harmonic analysis only shows the steady-state response and ignores all transient effects, while random vibration includes the total response including transient effects which is naturally unpredictable. Due to the transient effects being unpredictable, the random vibration results can only be a statistical solution. Additionally, random vibration will output a contour plot for directional deformation, but instead will be a statistical solution and will not show deformation in live form. These solutions are given a scale factor based on their probability, the factor values of interest are 1 sigma and 3 sigma. The 1 sigma is a 68.269% probability that the deformation in the selected direction will stay below a maximum value. Lastly, the 3 sigma factor is a 99.73% probability that the same deformation will stay below another certain value.

Table 7 Random Vibration MPE [24]

Frequency (Hz)	Random Vibration MPE, All Axes
20	0.01
50	0.015
700	0.015
800	0.03
925	0.003
2000	0.00644

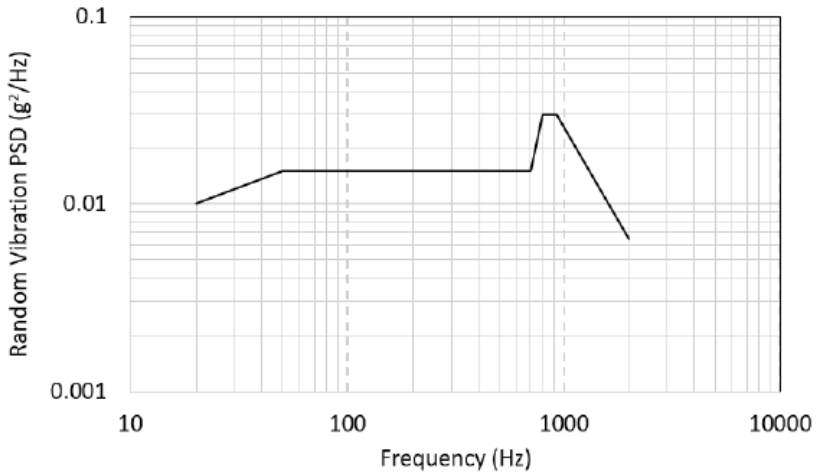

Figure 6.8 Random vibration maximum predicted environment [24]

6.5 Random Vibration Results

The results for random vibration include the 1 and 3 sigma probability scale factors. These values have been calculated in the lateral and axial directions. Figure 6.9 shows both the 1 and 3 sigma scale factors and find that there is a 66.269% probability that the deformation will remain below 0.000104 mm in the x axis, and a 99.73% probability that the deformation will remain below 0.000314 mm also in the x axis. Figure 6.10 shows the x axis PSD response vs frequency and figure 6.12 shows the same response for the y axis. The 1 and 3 scale factor for the y axis can be seen in figure 4.11 and shows a 66.269% probability that the deformation will remain below 0.0000579 mm and a 99.73% probability that the deformation will remain below 0.000174 mm in the y axis.

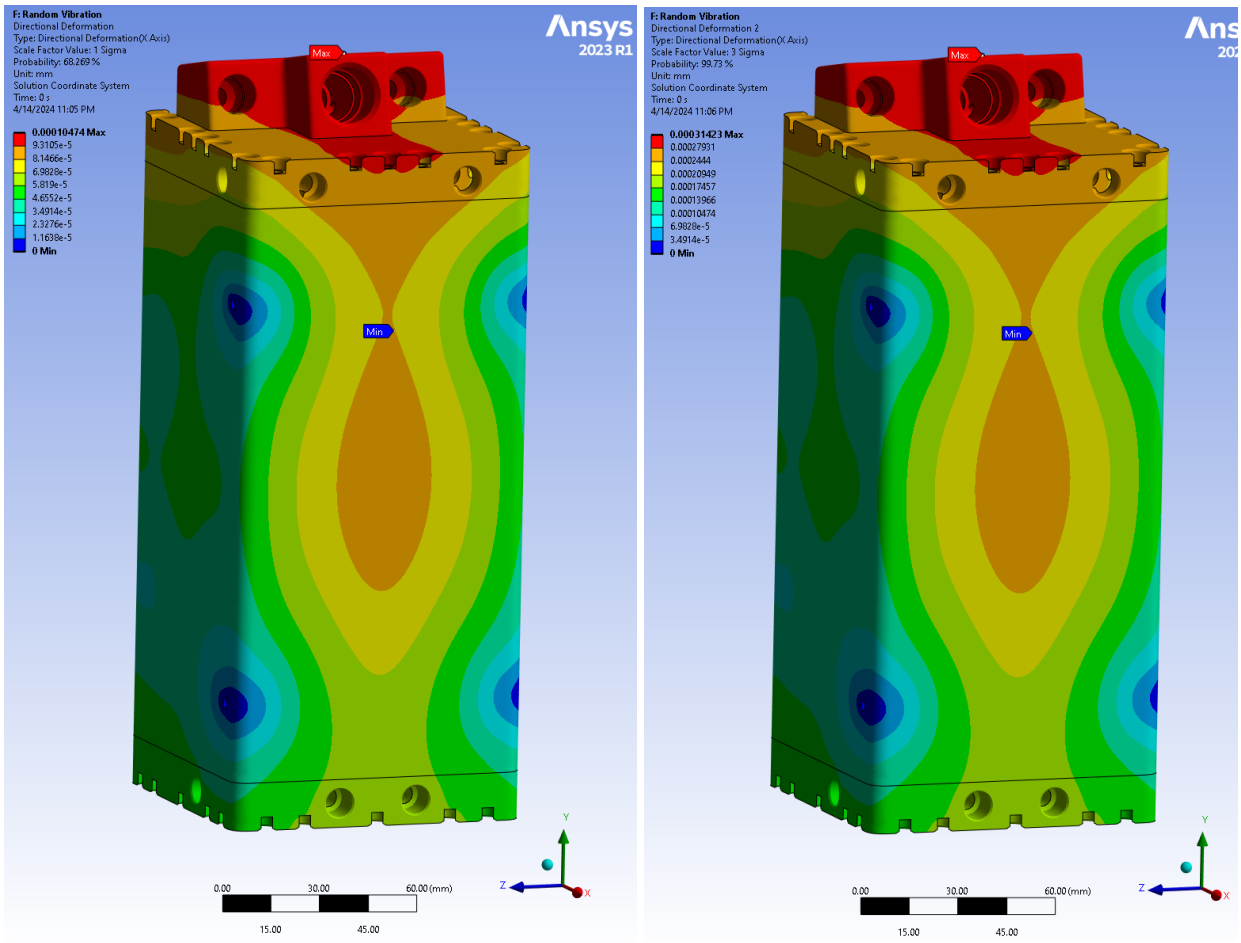

Figure 6.9 Random vibration x axis (lateral) deformation 1 sigma (left), 3 sigma (right)

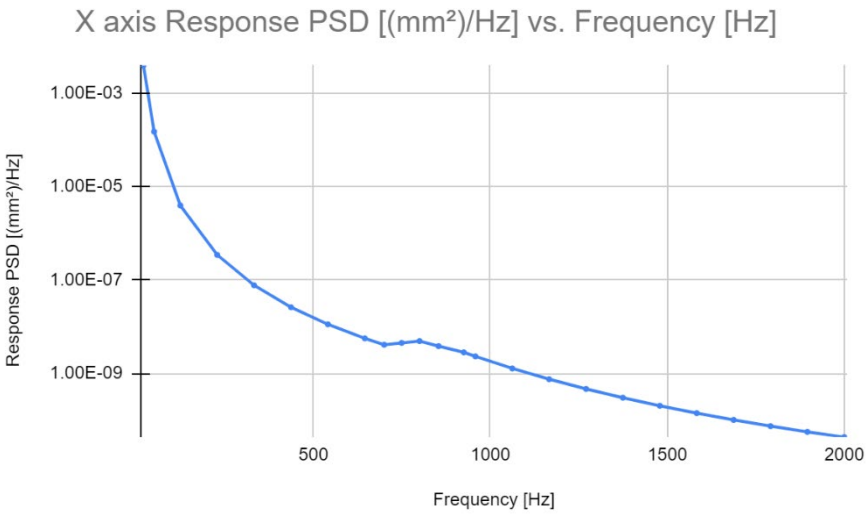

Figure 6.10 Frequency response psd vs. frequency for x axis (lateral)

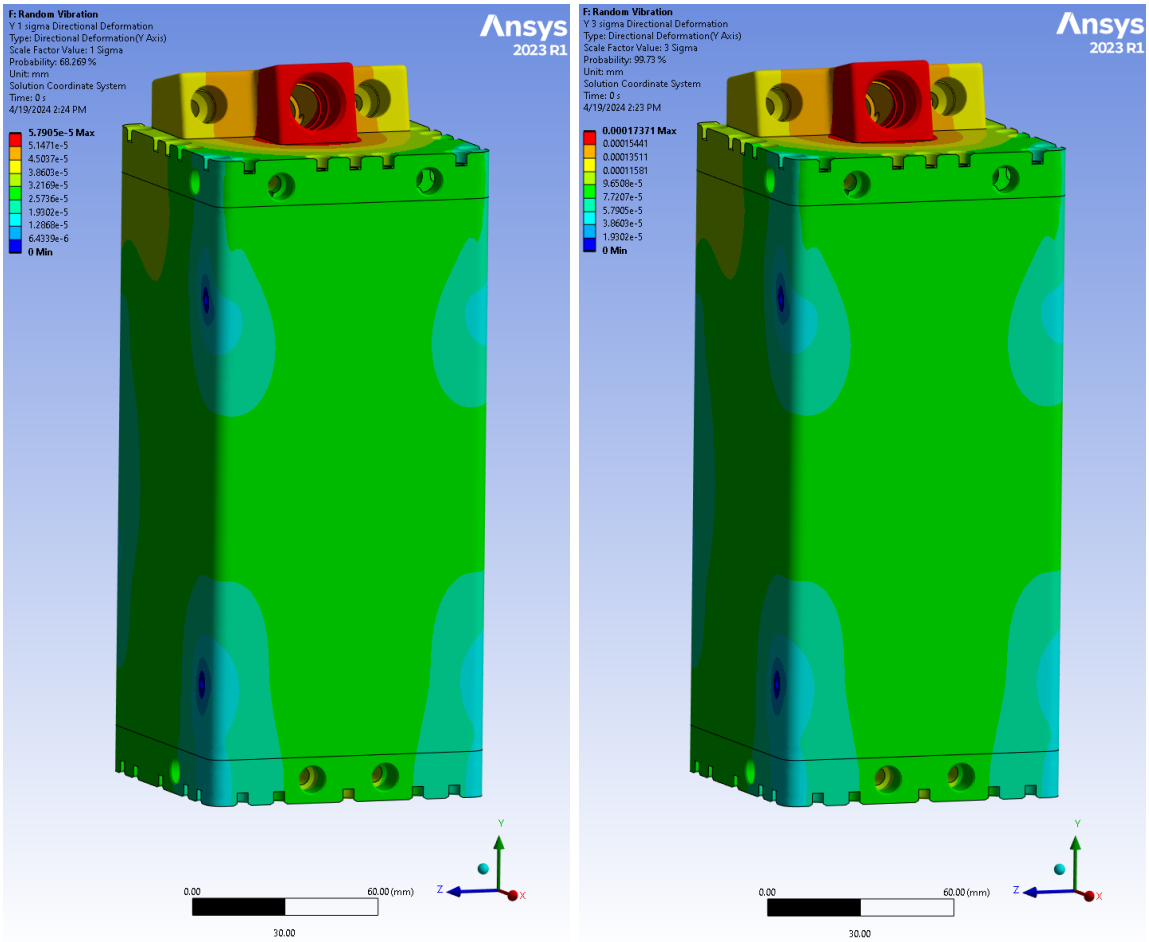

Figure 6.11 Random vibration y axis (axial) deformation 1 sigma (left), 3 sigma (right)

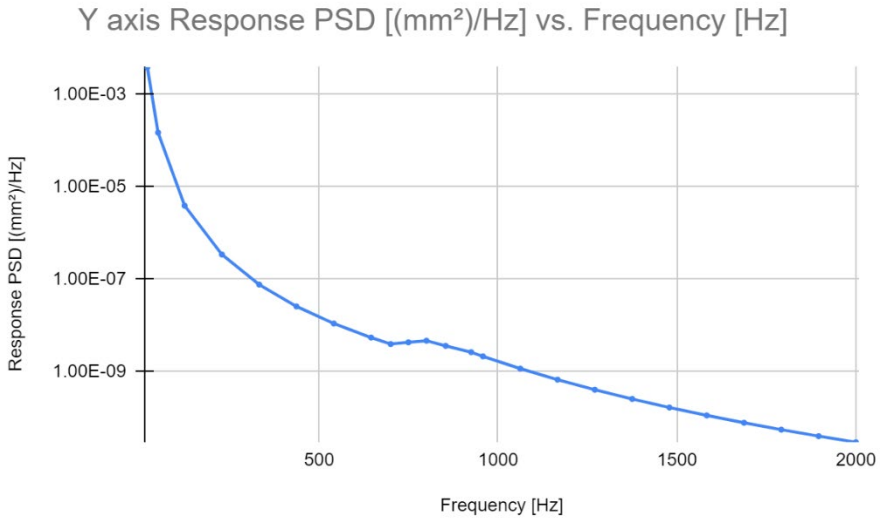

Figure 6.12 Frequency response psd vs. frequency for y axis (axial)

6.6 Random Vibration Analysis Results Discussion

From the results of the random vibration analysis, they must be compared to the Falcon 9 rideshare requirements to ensure system compliance. The system was subjected to a range of frequencies from 20 to 2000 Hz and maximum predicted environments of 0.0064 to 0.03 g acceleration. The results show that there is a 66.269% probability that the deformation will remain below 0.000104 and 0.0000579 mm for the x and y axis respectfully. Additionally, there is a 99.73% probability that the deformation will remain below 0.000314 mm and 0.000174 mm for the x and y axis respectfully. Comparing these deformations to the maximum deformation range of between 1.18 to 1.23% from section 2.1.2.2, which is the same process used in section 6.3, the results show the system could undergo a deformation of between 0.0000609 and 0.000330%. This is well below the maximum acceptance range which concludes that the system is ready for final qualification tests to prepare for integration and flight.

7. Concluding Summary

The goal of this project was to develop the geometry of a modular propellant tank for the use in a CubeSat of 6U to 12U. Over the course of the project, literature review was completed to show use cases for such devices in missions that have already been attempted which sent a CubeSat on missions such as to the Moon and Mars. System requirements from industry standards and the Falcon 9 launch vehicle were strictly followed to ensure the system could properly meet minimum requirements and ensure project success. This process involved conducting several forms of finite element analysis of the structure to obtain a highly accurate approximation of how the system reacts to internal and external conditions such as load factors.

7.1 Results Discussion

First, the system underwent modal analysis to predict the natural frequencies of the system to ensure the first mode frequency was above the minimum frequency from the launch vehicle. The launch vehicle required a natural frequency higher than 40 Hz and this system was found to have a mode 1 natural frequency of 4061.9 Hz. Second, the system was subjected to an internal working pressure of 750 psi using static structural analysis to verify that the system could withstand the expected operational pressure. With the calculated Von-mises stress that the geometry was expected to experience, the factor of safety was found by calculating the ratio between the maximum pressure and the operational pressure. This factor of safety ratio was found to be 1.9 which was within the requirements of 1.5 to 2.2.

Following the modal and structural analyses, the system was subjected to the external applied loads from the launch vehicle. These loads were found as a combined load from the Falcon 9 rideshare user guide and gave a value of 10 g's in the axial direction and 17 g's in the lateral direction. This load was an important aspect for the harmonic, or sine sweep, analysis which identified the frequencies that would cause the system to experience the highest amount of deformation. Harmonic analysis identified that the system would experience a lateral deformation of 0.003 mm at a frequency of 4249.7 Hz, and also an axial deformation of 0.003 mm at a frequency of 6523.8 Hz. Additionally, the system was subject to a frequency range of 20-2000 Hz and a maximum predicted environment from 0.0064 to 0.03 g's during the random vibrational analysis. This had the effect of causing a deformation of 0.0000609 and 0.000330% which is so low that it is basically negligible.

7.2 Lessons learned

Over the course of this project, many lessons were learned in CAD design and Finite Element Analysis. Many of these lessons were either small mistakes or changes that caused a large difference in the results, or purely learning a new method of analysis which was once foreign. Some of the small mistakes include originally sizing the outer dimensions of the propellant tank

to 100 mm, this is a problem because if this were to integrate into a CubeSat, then it would be the same width and not fit. The tank width was then decreased to 95 mm which made the wall thickness less and decreased the overall integrity of the tank. Although the tank structural integrity was decreased, the tank was still able to pass all of the analyses. An additional change that caused a large difference in the results was when manufacturing the tank, the machinists had requested to increase some of the inner radii of the corner pockets from 2 mm to 1/8 inch. This minor change in geometry caused a large structural integrity increase where the original burst pressure was about 875 psi and 2100 psi after. Thankfully, the addition of both of these changes ended up equaling out and left the final MEOP and safety factor to meet exactly within the requirements.

7.3 Next Steps/Future Work

For future work on the propellant tank, further analyses and tests will need to be completed to check all of the boxes for the Falcon 9 rideshare requirements. The analyses required include performing an acoustic test on the tank that closely simulates the acoustic environment that will be experienced during the entire flight envelope. Since this system is a pressurized propellant tank, the system must pass three pressure and leaks tests. These tests include a pressure system test which verifies the burst pressure of the system and confirms the safety ratio of operating pressure to burst pressure. The second and third tests are basically the same, one is a full system leak test, and the other is a leak test on only the pressure vessel. This requires the tank to be pressurized to the operational pressure and monitor the pressure drop per minute or hour. In addition to pressure drop, the tank can visually be checked for leaks by spraying water and soap mixture on fittings or mating areas of the parts. If there is a leak, it will be identified by the soap created bubbles at the source of the leak.

Another important required test of the system is the combined thermal and vacuum cycle test. This involves mounting the tank inside of a TVAC chamber which has the ability to simulate all environments of space. It uses high power vacuum and cryogenic pumps to pull a vacuum as close to $1x10^{-11}\ Torr$ as possible. This will test the system on how it will react once exposed to the vacuum of space. Additionally, the chamber is capable of either decreasing or increasing the temperature from -270°C to 120°C. This cycling of extreme cold to hot is a test of thermal expansion of the system which could highlight major issues with sealing or operation if the system didn't take expansion well enough into consideration.

References

[1] Johnstone, A., “CubeSat design specification,” Cubesat.org, 2022, URL: https://static1.squarespace.com/static/5418c831e4b0fa4ecac1bacd/t/62193b7fc9e72e0053f00910/1645820809779/CDS+REV14_1+2022-02-09.pdf [retrieved 17 September 2023].
[2] Shkolnik, E. L., “On the verge of an astronomy CubeSat Revolution,” Nature Astronomy, vol. 2, 2018, pp. 374–378, URL: https://www.researchgate.net/publication/324872683_On_the_Verge_of_an_Astronomy_CubeSat_Revolution [retrieved 23 September 2023].
[3] “Lunah-Map (lunar polar hydrogen mapper),” eoPortal, 2019, URL: https://www.eoportal.org/satellite-missions/lunah-map#spacecraft [retrieved 23 September 2023].
[4] “Lunar Flashlight,” NASA, URL: https://www.jpl.nasa.gov/missions/lunar-flashlight [retrieved 23 September 2023].
[5] Clark, P., “NASA - NSSDCA,” NASA Space Science Data Coordinated Archive, 2022, URL: https://nssdc.gsfc.nasa.gov/nmc/spacecraft/display.action?id=L-ICECUBE [retrieved 23 September 2023].
[6] “Mars Cube One (Marco),” NASA, URL: https://www.jpl.nasa.gov/missions/mars-cube-one-marco [retrieved 23 September 2023].
[7] Mahoney, E., “Nea Scout,” NASA, 2020 URL: https://www.nasa.gov/content/nea-scout [retrieved 23 September 2023].
[8] Nosseir, A. E., Cervone, A., and Pasini, A., “Modular impulsive green monopropellant propulsion system (MIMPS-G): For CubeSats in leo and to the Moon,” Aerospace, vol. 8, 2021, p. 169, URL: https://ui.adsabs.harvard.edu/abs/2021Aeros...8..169N/abstract [retrieved 23 September 2023].
[9] Huggins, G. M., Talaksi, A., Andrews, D., Lightsey, E. G., Cavender, D., McQueen, D., Williams, H., Diaz, C., Baker, J., and Kowalkowski, M., “Development of a CubeSat-scale green monopropellant propulsion system for NASA’s Lunar Flashlight Mission,” AIAA Scitech 2021 Forum, 2021, URL: https://www.ssdl.gatech.edu/sites/default/files/ssdl-files/papers/conferencePapers/AIAA-2021-1976.pdf [retrieved 23 September 2023].
[10] Krejci, D., and Lozano, P., “Space Propulsion Technology for small spacecraft,” Proceedings of the IEEE, vol. 106, 2018, pp. 362–378, URL: https://ieeexplore.ieee.org/abstract/document/8252908 [retrieved 25 September 2023].
[11] Porter, R. N., and Stanford, H. B., “Propellant expulsion in unmanned spacecraft,” SAE Technical Paper Series, 1964, URL: https://apps.dtic.mil/sti/citations/ADB209604 [retrieved 17 September 2023].
[12] Zhang, H., Gu, S., Zhang, J., Ouyang, R., Yu, B., Yang, W., and Zhang, X., “Development of titanium diaphragms for space propellant tank,” Journal of Physics: Conference Series, vol. 2336, 2022, p. 012002, URL: https://iopscience.iop.org/article/10.1088/1742-6596/2336/1/012002/meta [retrieved 24 September 2023].

[13] Wheeler, D. J., "By order of the commander space systems command manual space ... - AF," Air Force Space Command, 2019 URL: https://static.e-publishing.af.mil/production/1/ssc/publication/sscman91-710v3/sscman91-710v3.pdf. [retrieved 17 September 2023].
[14] "Falcon 9 Launch Guide" SpaceX, United States, 2009, URL: https://www.spacex.com/media/falcon-users-guide-2021-09.pdf [retrieved 23 September 2023].
[15] Magomedov, I. A., and Sebaeva, Z. S., "Comparative study of finite element analysis software packages," Journal of Physics: Conference Series, vol. 1515, 2020, p. 032073, URL: https://iopscience.iop.org/article/10.1088/1742-6596/1515/3/032073/meta [retrieved 23 September 2023].
[16] Lvovsky, O., Cobbs, R., Francis, R., and Ungar, E., "NASA-STD-7012 LEAK test requirements: Potential reference for ASNT ..." URL: https://ntrs.nasa.gov/api/citations/20190033156/downloads/20190033156.pdf [retrieved 24 September 2023].
[17] Lyu, Y., *Finite element method: Element solutions*, Singapore: Springer Nature Singapore, 2022, URL: https://www.slideshare.net/RAYCRISTIANQUICAAPOM/finite-element-method-element-solutions-by-yongtao-lyu-firts-editon-zlibrarypdf [retrieved 17 December 2023].
[18] Petyt, M., *Introduction to finite element vibration analysis*, New York, NY: Cambridge University Press, 2010, URL: https://www.cambridge.org/core/books/introduction-to-finite-element-vibration-analysis/4345EDA6046AF3D6BEC8FD29F00AD646 [retrieved 17 December 2023].
[19] Abdelal, G. F., Abuelfoutouh, N., and Gad, A. H., *Finite element analysis for satellite structures: Applications to their design, manufacture and testing*, London: Springer London, 2013, URL: https://www.researchgate.net/publication/292655609_Finite_element_analysis_for_satellite_structures_Applications_to_their_design_manufacture_and_testing [retrieved 17 December 2023].
[20] Zhao, J., "Basics of structural vibration testing and analysis," *Crystal Instruments* URL: https://www.crystalinstruments.com/basics-of-structural-vibration-testing-and-analysis [retrieved 17 December 2023].
[21] Arenas, J. P., and Margasahayam, R. N., "Noise and vibration of spacecraft structures," *Ingeniare. Revista chilena de ingeniería*, vol. 14, 2006, URL: https://www.redalyc.org/pdf/772/77225398008.pdf [retrieved 17 December 2023].
[22] Dhar, S., Karlowatz, G., Ungersboeck, E., and Kosina, H., "Numerical and analytical modeling of the high-field electron mobility in strained silicon," *2005 International Conference On Simulation of Semiconductor Processes and Devices*, 2005, URL: https://www.researchgate.net/publication/4205218_Numerical_and_Analytical_Modeling_of_the_High-Field_Electron_Mobility_in_Strained_Silicon [retrieved 31 December 2023].
[23] Malkus, D. S., Plesha, M. E., Cook, R. D., and Witt, R. J., *Concepts and applications of finite element analysis*, New York, NY: John Wiley & Sons, 1989,

https://cybertycoons.files.wordpress.com/2014/04/robert_d-_cook_david_s-_malkus_michael_e-_pleshbookos-org-fem.pdf [retrieved 1 January 2024].
[24] “Rideshare Payload User’s Guide” SpaceX, United States, 2023, URL: https://storage.googleapis.com/rideshare-static/Rideshare_Payload_Users_Guide.pdf [retrieved 21 February 2024].